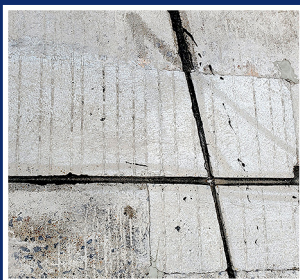
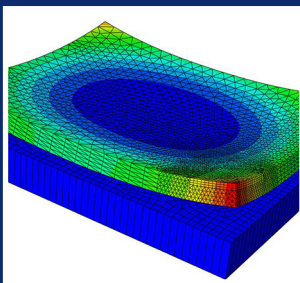
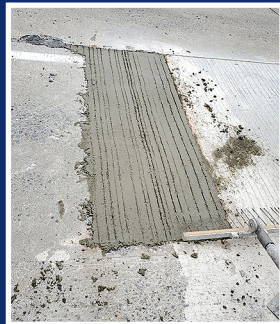


Material Compatible Repairs (MCRs) for Concrete Pavements and Bridge Decks

Summary Report

March, 2020



IRISE Consortium

Impactful Resilient Infrastructure
Science and Engineering

PITT | IRISE

Technical Report Document Page

1. Report No: IRISE-20-P19-02-01	2. Report Date: March, 2020
3. Report Title: Material Compatible Repairs (MCRs) for Concrete Pavements and Bridge Decks	4. Authors: Naser P. Sharifi, Steven G. Sachs, Julie M. Vandebossche, Max T. Stephens
5. Performing Organization Name and Address Department of Civil & Environmental Engineering 742 Benedum Hall University of Pittsburgh Pittsburgh, PA 15261	6. Sponsoring Organization Name and Address: IRISE Department of Civil & Environmental Engineering, 742 Benedum Hall University of Pittsburgh Pittsburgh, PA 15261
7. Abstract: Partial-depth repairs are a rehabilitation method commonly performed on concrete pavements and bridge decks to restore the integrity of the structure. However, in the past, partial-depth repairs have not always achieved their expected life. Some contributing factors include poor construction practices and the use of nondurable repair materials. Another consideration not previously considered is the compatibility between the in-situ concrete and the repair material. Additional stress is generated at the interface between the repair material and the existing concrete when the two materials deform at differently rates. This has the potential to occur when the elastic modulus, thermal coefficient of expansion and/or the drying shrinkage of the repair material is significantly different from that of the existing concrete. The focus of this study is on investigating the effects of the incompatibility between the repair and existing concrete through a laboratory investigation and a computational study. Then a methodology was established for developing a performance engineered repair material (PERM) to be used for performing a material compatible repair (MCR). This is accomplished through the proper selection of a coarse aggregate so that stiffness and thermal compatibility between the repair material and the existing concrete is assured. Internal curing was also investigated to reduce the drying shrinkage of the repair material to minimize the potential for debonding between the repair and the older existing concrete.	
8. Key Words: Material compatible repairs (MCR), Performance engineered concrete repair mixture (PERM), Partial-depth repairs, concrete pavements, Internal curing, Thermal compatibility	9. Distribution: Report available at: https://www.engineering.pitt.edu/Sub-Sites/Consortiums/IRISE/Content/Achievements/Products/

Material Compatible Repairs (MCRs) for Concrete Pavements and Bridge Decks

March 2020

Authors

Naser P. Sharifi, Ph.D., University of Pittsburgh

Steven G. Sachs, Ph.D., University of Pittsburgh

Julie M. Vandenbossche, Ph.D., P.E., University of Pittsburgh

Max T. Stephens, Ph.D., University of Pittsburgh

Technical Reviewers

Michael Burdelsky, P.E., Allegheny County

Jason Molinero, P.E., Allegheny Count

Jennifer Albert, Ph.D., P.E., Federal Highway Administration

Jonathan Buck, P.E., Federal Highway Administration

Pat Baer, Pennsylvania Department of Transportation



IRISE

The Impactful Resilient Infrastructure Science & Engineering consortium was established in the Department of Civil and Environmental Engineering in the Swanson School of Engineering at the University of Pittsburgh to address the challenges associated with aging transportation infrastructure. IRISE is addressing these challenges with a comprehensive approach that includes knowledge gathering, decision making, material durability and structural repair. It features a collaborative effort among the public agencies that own and operate the infrastructure, the private companies that design and build it and the academic community to develop creative solutions that can be implemented to meet the needs of its members. To learn more, visit: <https://www.engineering.pitt.edu/irise/>.



Acknowledgements

The authors gratefully acknowledge the financial support of all contributing members of IRISE. The authors also would like to thank Golden Triangle Construction for providing technical information regarding accelerated-setting concrete repairs. Specifically, we are indebted to the advice and assistance provided by Mr. Chip Dalesandro of Golden Triangle Construction, who shared his expertise in performing field installations of partial depth repairs and provided a very informative tour of their project. The authors would also like to thank Northeast Solite Corporation for supplying Lightweight Aggregate, Bryan Materials Group for supplying sand and coarse limestone, Cemex Corporation for supplying cement, Sika Group for supplying chemical admixtures, and Evonik Industries for supplying the Superabsorbent Polymers. In addition, we are indebted to the advice and assistance provided by Mr. Mike Burdelsky and Mr. Jason Molinero of Allegheny County, Ms. Jen Albert and Mr. Jon Buck of Federal Highway Administration, and Ms. Pat Baer of Pennsylvania Department of Transportation.

Disclaimer

The views and conclusions contained in this document are those of the authors and should not be interpreted as representing official policies, either expressed or implied, of the Pennsylvania Department of Transportation, the Pennsylvania Turnpike Commission, Allegheny County, Golden Triangle Construction, or Michael Baker In

Table of Contents

1 Introduction.....	1
1.1 Background.....	1
1.2 Problem Statement.....	3
1.3 Research Plan.....	3
2 Identification of Key Material Properties.....	5
3 Internal Curing Agents.....	7
3.1 Lightweight Aggregate.....	8
3.2 Super Absorbent Polymers.....	8
3.3 Cellulose Fibers.....	8
4 Laboratory Experiment.....	9
4.1 Material Selection and Test Methods.....	9
4.1.1 <i>Material Selection</i>	9
4.1.2 <i>Mixture Designs</i>	11
4.1.2.1 <i>General Mixture Proportioning</i>	11
4.1.2.2 <i>Internal Curing Agents</i>	12
4.1.3 <i>Test Methods</i>	14
4.1.3.1 <i>Fresh Concrete Properties</i>	14
4.1.3.2 <i>Compressive Strength</i>	15
4.1.3.3 <i>Modulus of Elasticity</i>	16
4.1.3.4 <i>Bond Strength: Slant Shear</i>	17
4.1.3.5 <i>Bond Strength: Splitting Tensile</i>	18
4.1.3.6 <i>Coefficient of Thermal Expansion</i>	19
4.1.3.7 <i>Shrinkage</i>	21
4.2 Results and Discussion of Laboratory Experiments.....	22
4.2.1 <i>Compressive Strength</i>	22
4.2.2 <i>Modulus of Elasticity</i>	23
4.2.3 <i>Bond Strength: Slant Shear</i>	25
4.2.4 <i>Bond Strength: Splitting Tensile</i>	26
4.2.5 <i>Coefficient of Thermal Expansion</i>	28
4.2.6 <i>Shrinkage</i>	30

5 Numerical Modeling 33

5.1 Model Development..... 33

5.2 Loading Scenarios..... 35

5.3 Results and Discussion of Computational Simulations 38

6 Implementation Plan 44

6.1 Practical Considerations and Obstacles 44

6.2 Methodology for Developing a PERM for an MCR..... 46

7 Conclusion and Future Work 48

8 Appendix (Statistical Analysis Details) 49

9 References 50

Nomenclature

MCR	Material compatible repairs
PERM	Performance engineered concrete repair material
CTE	Coefficient of thermal expansion ($\mu\epsilon/^\circ\text{F}$)
E	Modulus of elasticity (psi)
k-value	Modulus of subgrade reaction (psi/in)
C	Base/slab frictional restraint factor (1)
ϵ	Shrinkage ($\mu\epsilon$)
w/c	Water to cement ratio (by weight)
C_f	Cement factor for concrete mixture (lb/yd ³)
CS	Chemical shrinkage of cement (oz. of water/oz. of cement)
α_{max}	Maximum expected degree of hydration of cement (1)
IC	Internal curing
LWA	Lightweight aggregate
S	Saturation degree of LWA (1)
ϕ_{LWA}	Water absorption capacity of LWA (lb water/lb dry LWA)
SAP	Superabsorbent polymers
AEA	Air entraining admixture
SP	Superplasticizer
AA	Accelerating admixture

1 Introduction

1.1 Background

Partial-depth repairs are between the rehabilitation methods that have been commonly performed on concrete pavements and bridge decks. Partial-depth repairs restore structural integrity and can improve ride quality, especially if performed in conjunction with diamond grinding. Repairs of partially deteriorated joint areas also restore a well-defined, uniform joint-sealant reservoir prior to joint resealing [1]. PennDOT Publications 408 and 242 provide specifications for the repair of damaged concrete pavements. In general, there are three scenarios which require the use of a concrete repair mixture in damaged concrete pavements: dowel retrofit, partial depth pavement repair, and full depth pavement repair. Dowel retrofit is used to improve load transfer between joints or cracks through the installation of new dowels. In this procedure, dowels are placed within slots created parallel to the roadway centerline, and the slots are filled with a concrete patching material, which is vibrated thoroughly to consolidate material within the slots and around the new dowel bars (Figure 1.a).

Partial depth repair is discussed in Sections 525 and 4.4 of Publications 408 and 242 respectively [2], [3]. Partial depth repairs are used on transverse or longitudinal joints, cracks, and interior slab spalls when the depth of the repair is no greater than half the slab thickness (Figure 1.b). Partial depth repairs are broken into two categories: Type 1- spot repairs between 15" and 6' in length and Type 2- extended repairs for lengths greater than 6'. In the partial depth repair procedure, deteriorated concrete is removed from the damaged region within the repair area to a minimum depth of 2", and the repair material is placed in the prepared region.



Figure 1. Concrete pavement repair types. a) Dowell retrofit, b) Partial-depth repair, c) Full-depth repair [2], [3]

PennDOT Publications 408 and 55 provide specifications and recommendations for the rehabilitation of concrete bridge decks, too [2], [4]. Section 1040 of Publication 408 classifies bridge deck repair into three categories: Type (1) – areas where deteriorated concrete extends to a maximum depth of the top of the top mat of reinforcing bars with no more than one-quarter of the bar diameter exposed (Figure 2.a). Type (2) - areas where deteriorated concrete extends beyond the depth of the top of the top mat of reinforcement bars or where reinforcement bars are unbonded (Figure 2.b). Type (3) – areas where deteriorated concrete or patching extends to the full depth of the deck (Figure 2.c). In each case, deteriorated concrete is removed from the deck, the repair region is cleaned and coated with concrete bonding compound, and the patching material is placed in the prepared region.



Figure 2. Concrete bridge deck repair types. a) Deteriorated concrete extends to the depth of top of the reinforcing bars, b) Deteriorated concrete extends beyond the depth of top of the reinforcing bars, c) Deteriorated concrete extends to the full depth of the deck [2], [3]

Publication 408, Section 525 “Concrete Pavement Partial-Depth Repair” categorizes the partial depth concrete repair materials into three main classes: Class AA Cement Concrete, Modified; Class AA Cement Concrete, Accelerated; and Rapid-Set Concrete Patching Material. Details regarding the requirements of each of these repair material classes are provided in Publication 408, Section 704 and Section 525.2. It should be mentioned that the repair material developed in this study is a Class AA-Accelerated cement concrete repair. A primary requirement for this class of repair material is 7-hour compressive strength, which needs to be at least 1,500 psi. Based on Section 704 of Publication 408, the patching material for concrete bridge decks is a Class AAAP Cement Concrete. Some of the mixture criteria of the Class AA and the Class AAAP repair materials, such as the maximum allowable cement factor, are different. This difference, however, does not change the procedure that was proposed in this report to develop MCRs.

1.2 Problem Statement

Premature failures in partial depth repairs can be caused by poor construction practices and durability issues. Other issues include: compressive failure of the repair material, variability in the repair material, insufficient consolidation in the repair, incompatible thermal expansion between the repair material and existing concrete, autogenous shrinkage in the repair material, delayed curing, premature loading, and inclement weather during or after repair [5]. The repair-specific concrete mixture designs specified in Publication 408 have been modified to address several of these deficiencies, however ongoing long-term performance issues in concrete pavement and bridge repair materials have been specifically identified by local bridge engineers [6], [7].

When it comes to partial depth repairs, one of the key factors that contribute to the premature failure of the repair section is the incompatibility in deformation between the in-situ concrete and repair material. The in-situ concrete and the repair section should respond as a monolithic section. Stiffness incompatibility leads to unequal deformations under mechanical loads, which leads to the development of additional stresses in the materials and along the contact interface. Thermal incompatibility leads to unequal deformations under thermal loads. This also leads to the development of additional stresses in the materials and the along contact interface. Finally, drying shrinkage of the repair material builds up stresses that are comparable, or even higher than, the mechanically and thermally induced stresses. These incompatibility problems, along with the excessive shrinkage of repair material, could expedite the failure of partial-depth repairs. Therefore, special consideration should be given to the compatibility between the existing concrete and the repair material when developing the mixture design for the repair material.

1.3 Research Plan

This study focuses on the performance of partial depth repairs from a material point of view. In order to increase the service life of partial depth repairs, it is critical to first identify distress mechanisms and parameters that speed up the failure, then adopt best practices to control these mechanisms. Doing so increases the service life of pavements, improves the ride quality, increases safety, decreases closure time, and reduces costs and material consumption.

The primary focus of this study was on the development of a repair material that is compatible with the in-situ concrete. To do so, first locally available coarse aggregates, that could be used to achieve stiffness and thermal compatibility between the repair material and the existing concrete, were identified. This also included identifying sources of lightweight aggregates (LWA) capable of providing internal curing to minimize drying shrinkage of the repair material. Then, these materials were used to develop different mixture designs; and a comprehensive laboratory investigation was performed to establish the properties of the developed MCRs. Next, a computational model was developed to evaluate the performance of the MCRs for a range of vehicle and environmental loading conditions.

This report consists of five main parts. In the first part (Section 2), the key compatibility properties of partial depth repairs are identified. In the second part (Section 3), the concept of internal curing is explained, and the three main internal curing agents are discussed. The third part (Section 4) is devoted to the development of MCRs through a comprehensive laboratory study. In the fourth part (Section 5), the performance of concrete repair mixtures under different load conditions is evaluated through a computational study. The effects of incompatibility between the in-situ concrete and repair material, as well as the effects of incorporating internal curing agents, on the induced stresses are also studied in this section. Finally, in the fifth part (Section 6), the feasibility of implementing an MCR and potential obstacles are discussed, and the concept of a performance engineered concrete repair mixture (PERM) is identified.

2 Identification of Key Material Properties

The main stresses that a concrete slab or a repair section experiences during its service life are induced from traffic loads, changes in temperature, shrinkage, etc. In order to prevent the generation of excessive stresses in the concrete slab, the repair section, and the interface under traffic loads, it is necessary that the stiffness of the repair material match the in-situ concrete stiffness. On the other hand, to prevent the development of additional stresses under thermal loads, the thermal properties of the repair material should be compatible with the in-situ concrete. In addition, the shrinkage of the repair material should be controlled to hinder the failure of repair section. Therefore, modulus of elasticity (E), coefficient of thermal expansion (CTE), and long-term shrinkage of repair material are the three main parameters that play the key role in achieving the desired compatibility between the repair material and the in-situ concrete.

Concrete is a composite material, and its mechanical and thermal properties are driven from its ingredients. Therefore, in order to achieve the desired thermal and mechanical properties for the repair material, each of the components of the mixtures should be judiciously selected and the mixture design should be engineered. Table 1 summarizes the relationship between different mixture design parameters (e.g. the w/c, aggregate properties, etc.) and characteristics of the repair materials that will be investigated in this study (E , CTE, shrinkage, etc.). The importance level of each of the parameters in Table 1 is classified based on the following discussions:

- Water to cement ratio (w/c) significantly affects the strength, stiffness, and shrinkage performance of the mixture. Higher w/c decreases the concrete strength and stiffness, and increases the short- and long-term shrinkages [8]. However, compared to other components, it has a minor effect on the CTE of the concrete.
- The coarse aggregate volume percentage of the mixture is higher than any other component (70% to 80% of the total volume of the concrete) [8]. Therefore, the physical and thermal properties of the coarse aggregate significantly affect the strength, stiffness, and CTE of the repair material. Coarse aggregate also affects shrinkage performance; however, the effect is minor relative to that of an internal curing agent. Internal curing is a technique to reduce the drying shrinkage of concrete. Discussions regarding internal curing are provided in another

section. The main internal curing agents consist of lightweight aggregate (LWA), superabsorbent polymers (SAPs), or cellulose fibers (CFs).

- The volume percentage of LWA when used for internal curing is usually limited to a small fraction of fine aggregate [9]. Similarly, the volume fraction of SAPs and CFs is very low compared to other mixture components. Therefore, compared to coarse aggregate, the properties of the internal curing agents play a minor role in the strength, stiffness, and CTE of the mixture. However, they significantly affect the short- and long-term shrinkages of the mixture [9].
- Liquid additives should not play a significant role in the hardened properties of the compatible repair material. However, they will be used to achieve other performance criteria such as setting time and workability.

Table 1. Correlation between concrete components and mechanical, physical, and thermal properties of repair material (significant effect: xxx, minor effect: x)

Mixture component	Performance criteria					
	Strength	Compatibility			Fresh concrete	
		E ²	CTE ³	Shrinkage	Set time	Slump
Cement paste (cement type, w/c ¹)	xxx	xxx	x	xxx	Shall be modified by incorporating additives. (Section 4.1.2)	
Coarse aggregate	xxx	xxx	xxx	x		
Internal curing agent (LWA ⁴ , SAP ⁵ , CF ⁶)	x	x	x	xxx		

¹ Water to cement ratio

² Modulus of elasticity

³ Coefficient of thermal expansion

⁴ Lightweight Aggregate

⁵ Super absorbent polymers

⁶ Cellulose fibers

The mechanical and thermal properties of aggregates that are commonly used in concrete fall within a wide range. Depending on the type, the aggregate can have a high, moderate, or low elastic modulus and CTE. In addition, some of the key parameters of LWA, such as the water absorption capacity, greatly depends on the aggregate source. Therefore, to better understand the effect of material sources on the stiffness, CTE, and shrinkage performance of the repair material, various mixtures, which contain aggregates from different sources will be evaluated.

3 Internal Curing Agents

Internal curing is a curing mechanism by which hydration is constantly supplied to the cementitious matrix after curing by incorporating saturated aggregates or other porous or absorptive materials to the mixture [10]. In internal curing mixtures, the saturated materials act as reservoirs from which the cement can continue to draw water after the free water is depleted, thereby providing distributed hydration and limiting autogenous shrinkage (Figure 3) [9]. Using internal curing in repair mixtures can result in an improved bond between the repair material and existing concrete, which can extend the life in repair applications. It can also potentially reduce drying shrinkage [11].

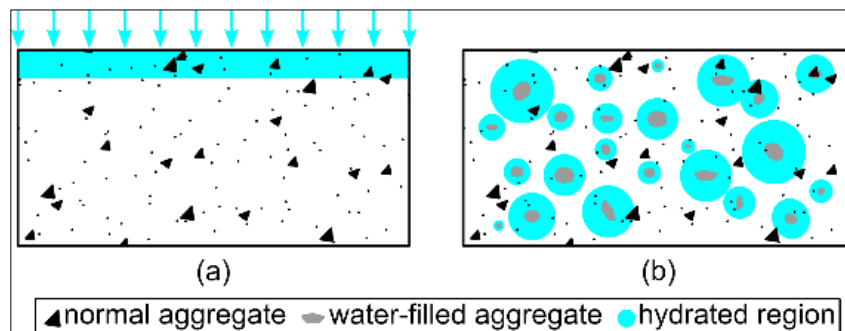


Figure 3. a) External curing, b) Internal curing (adopted from [12])

Although very limited work has been performed to investigate internal curing for use in rapid repair materials, internal curing mixtures have previously been implemented in concrete pavement and bridge deck applications [9]. An internal curing mixture was developed by the Texas Department of Transportation for use in concrete pavements. The mixture was designed to achieve a minimum compressive strength of 3,500 psi at 7-days and was employed in a continuously reinforced concrete pavement. The pavement exhibited a significant reduction in cracks relative to traditional concrete pavement mixtures, and has maintained a high strength and stiffness.

Internal curing mixtures have also been implemented in bridge decks in New York, Ohio, and Indiana [9], [13]. The mixture designs used in each state varied, however in each case, some percentage of traditional aggregate was substituted for saturated light weight aggregate, which acted as the internal curing agent. In all cases, the strengths of the internally cured mixtures were comparable to that of conventional concrete, and bridges with internally cured mixtures in Indiana are expected to have a significantly longer service life than bridges with conventional bridge deck

materials [13]. The Ohio and New York Departments of Transportation have yet to quantify the long-term benefits of using internal curing mixtures in bridge decks [9].

In the following sections, three main internal curing agents, i.e. LWA, SAP, and SF, are introduced; however, in this study, only LWA and SAP were used as the internal curing agent in the repair materials.

3.1 Lightweight Aggregate

Lightweight aggregate has been widely used as an effective internal curing agent. These aggregates can be found naturally (e.g. pumice and puerlite) or can be artificially created by super-heating raw materials (e.g. clay, shale, slate, blast furnace slag) to increase porosity. LWA is shown to have excellent internal curing properties due to their high water carrying capacity [14]. They are also compatible with other concrete ingredients. Using LWA for internal curing is shown to reduce drying and autogenous shrinkages [9], [13], [15], [16].

3.2 Super Absorbent Polymers

Super absorbent polymers (SAPs) have the ability to absorb a large amount of liquid from the surroundings and retain it within their structure. This makes them ideal internal curing agents, that have been demonstrated to significantly reduce drying shrinkage and cracking [17]. Internal curing mixtures with SAP have also been shown to increase durability when exposed to multiple freeze/thaw cycles, as the voids left after the SAPs dehydrate, which allows for the expansion of water. There are various types of SAPs commercially available [18].

3.3 Cellulose Fibers

Cellulose fibers (e.g. wood fibers) have also been suggested for use in internal curing mixtures [19]. The fibers are prepared by shredding wood materials to a size of approximately 0.1" and applying an alkaline resistant coating. The fibers are then fully saturated and introduced into the concrete mixture by adding them to the mix water to increase dispersion.

4 Laboratory Experiment

4.1 Material Selection and Test Methods

4.1.1 Material Selection

Type I Ordinary Portland Cement (OPC), produced by CEMEX®, with a specific gravity of 3.15 and in accordance to ASTM C150 “Standard Specification for Portland Cement” and AASHTO M85 “Standard Specification for Portland Cement” requirements was used. The cement had an initial setting time of 120 min, final setting time of 240 min, Blaine fineness of 1,963 ft²/lb, and normal consistency of 25.7%.

Two types of coarse aggregate, one type of fine aggregate (ordinary sand), and one type of lightweight aggregate (LWA) were selected (Figure 4). The coarse aggregates were #8 limestone and #8 quartzite. Limestone has been widely used for pavement applications in Pennsylvania. Quartzite is also used for pavement applications; however, some of its physical characteristics are significantly different from limestone. Selecting these two aggregates makes it possible to investigate how using aggregates with different characteristics affects the physical and mechanical properties of concrete.

Based on Publication 408 specifications, for Class AA-Accelerated cement concrete repair, the coarse aggregate must be #8 aggregate. Grading requirements for coarse aggregates are provided in ASTM C33 “Standard Specification for Concrete Aggregates.” The utilized #8 aggregates meet the requirements provided in this standard. The LWA was a fine expanded shale manufactured by Northeast Solite Corporation. The physical properties of the aggregates are presented in Table 2, and their particle size distribution are depicted in Figure 5. The sieve analysis of the aggregates was conducted based on ASTM C136 “Standard Test Method for Sieve Analysis of Fine and Coarse Aggregates” specifications.



Figure 4. Aggregates. a) #8 Limestone, b) #8 Quartzite, c) Sand, d) Fine LWA

Table 2. Physical properties of the aggregates

Aggregate	Specific gravity	Water absorption	Source
#8 Limestone	2.70	0.51%	Bryan Materials Group
#8 Quartzite	2.59	0.72%	New Enterprise Stone & Lime Co.
Sand	2.62	1.24%	Bryan Materials Group
LWA	1.65	18.5%	Northeast Solite Corporation

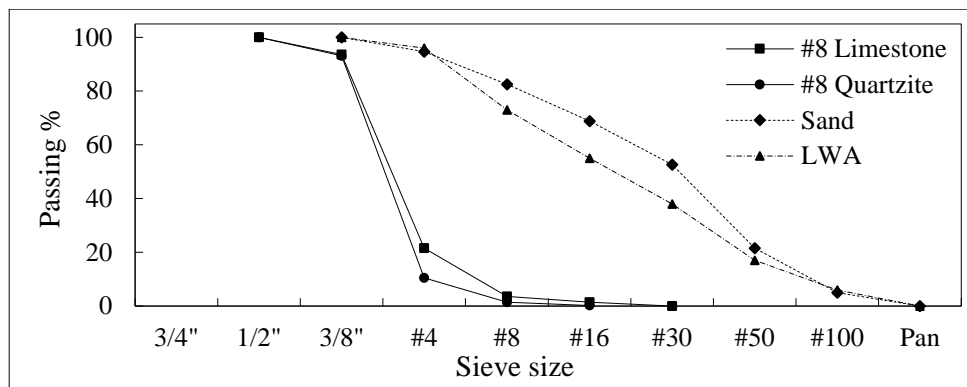


Figure 5. Sieve analysis of the aggregates

In addition to LWA, one type of super absorbent polymer (SAP) was used as the internal curing agent in the concrete mixtures. The utilized SAP was Stockosorb SW, provided by Evonic Industries®, which is an acrylic acid-co-acrylamide polymer (Figure 6). Considering the high pH of the cement pore solution, these types of polymers show a better performance compared to acrylic acid polymers. The diameter of Stockosorb SW particles was mostly between 200 μm and 800 μm, and its specific gravity was approximately equal to 0.6.

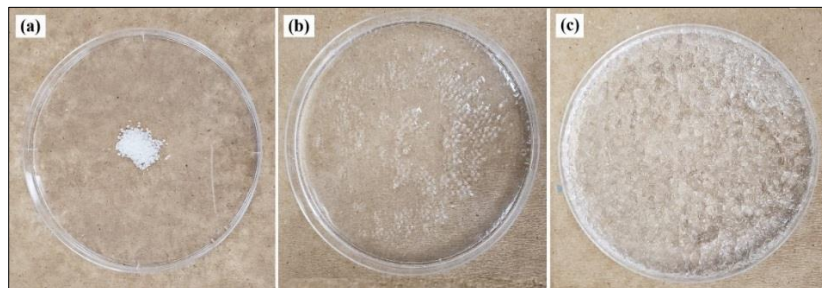


Figure 6. Superabsorbent Polymer. a) Dry powder, b) Thirty seconds after adding water, c) Three minutes after adding water

Three types of admixtures were used in the mixtures to meet the targeted air content, workability, and early-age compressive strength. Sika[®] Air-260, Sika[®] ViscoCrete-1000, and SikaSet[®] NC were used as the air entraining admixture (AEA), super plasticizer (SP), and accelerating admixture (AA), respectively. The specific gravity of the admixtures are equal to 1.01, 1.06, and 1.37, respectively. It should be mentioned that SikaSet[®] NC is a non-chloride accelerating admixture, and all admixtures meet the requirements of ASTM C494 “Standard Specification for Chemical Admixtures for Concrete.”

4.1.2 Mixture Designs

4.1.2.1 General Mixture Proportioning

Five different concrete mixtures were prepared. Mix L-NIC contained #8 limestone as the coarse aggregate, and no internal curing agent. Mix Q-NIC contained #8 quartzite as the coarse aggregate, and no internal curing agent. Mix L-SAP contained #8 limestone as the coarse aggregate, and SAP as the internal curing agent. Mix L-LWA contained #8 limestone as the coarse aggregate, and presoaked LWA as the internal curing agent. Finally, Mix Q-LWA contained #8 quartzite as the coarse aggregate, and presoaked LWA as the internal curing agent. This design matrix makes it possible to study the effect of incorporating different types of coarse aggregate on the modulus of elasticity and the coefficient of thermal expansion of concrete. In addition, it allows evaluation of the effectiveness of different internal curing agents in reducing the shrinkage of repair materials.

Details regarding the mixture designs, and the acceptable range for each property, specified by Publication 408 and ASTM C928 “Standard Specification for Packaged, Dry, Rapid-Hardening Cementitious Materials for Concrete Repairs,” are presented in Table 3. The mixture proportions and targeted values were kept constant for all five mixtures. The required 7-hr compressive strength for Class AA-Accelerated cement concrete repair is 1,500 psi based on Publication 408 specifications, which is a relatively high value. To meet this requirement, the highest allowable cement factor and a relatively high accelerating admixture dosage was used in all the mixtures. In addition, the water to cement ratio was kept as low as 0.30. The low w/c required the use of

relatively high dosages of superplasticizer and air entraining admixture to reach to the targeted slump and air content percentage, respectively.

Table 3. Mixture design

Proportion	Unit	Acceptable range		Actual value
w/c	by mass		< 0.42	0.30
Cement factor	lb/yd ³	Pub 408 specifications	588 – 800 ¹	800
Coarse Agg. / Concrete	ft ³ /yd ³		9.93 - 13.1	10.0
Coarse Agg. / Fine Agg.	by mass		-	1.24 - 1.42
Air entraining admixture	oz. / 100 lb cement	Product data sheet recommendation	0.1 - 6	5.5 ²
Superplasticizer	oz. / 100 lb cement		2 - 12	9.0*
Accelerating admixture	oz. / 100 lb cement		20 - 80	70
Targeted value				
Slump	Inches	ASTM C928	≥ 3	3
Air content	Percent	Pub 408	6	6

¹ This value is 560 to 690 lb/yd³ for class AAAP repair materials used for the repair of concrete bridge decks.

² For Mix L-SAP, where SAP was incorporated in the mixture, the dosages of air entraining admixture and superplasticizer were slightly reduced to achieve the targeted air content and slump (Table 4). This was because the incorporation of the SAP and additional water slightly increases the air content and workability of the concrete, thus a lower air entraining admixture and superplasticizer dosage is needed to achieve similar results.

4.1.2.2 Internal Curing Agents

The total required LWA to provide sufficient internal curing for the bulk cement paste is a function of the mixture cement factor, chemical shrinkage of the cement, maximum degree of hydration of the cement, and the properties of the LWA. The following equation is commonly used to determine the mixture proportioning of LWA [20]:

$$M_{LWA} = \frac{C_f \times CS \times \alpha_{max}}{S \times \Phi_{LWA}} \quad (1)$$

where M_{LWA} is the mass of dry fine LWA needed per unit volume of concrete (lb/yd^3), C_f is the cement factor for the concrete mixture (lb/yd^3), CS is the chemical shrinkage of the cement ($\text{oz. of water}/\text{oz. of cement}$), α_{\max} is the maximum expected degree of hydration of the cement, S is degree of saturation of the LWA, and ϕ_{LWA} is the water absorption capacity of the LWA ($\text{lb water}/\text{lb dry LWA}$).

For all mixes, C_f was equal to $800 \text{ lb}/\text{yd}^3$, and the chemical shrinkage of Type I cement is approximately equal to $0.055 \text{ oz.}/\text{oz.}$ [21], [22]. For a w/c below 0.36, the maximum expected degree of cement hydration was estimated as $[w/c]/0.36$ [20]. ϕ_{LWA} was reported by the manufacturer to be equal to $0.185 \text{ lb}/\text{lb}$, and after 24 h soaking in water, the degree of saturation of LWA was assumed to be equal to 1.0. Considering these values, the incorporated LWA in Mix L-LWA and Mix Q-LWA were equal to $197 \text{ lb}/\text{yd}^3$. It should be mentioned that when fine LWA was used as the internal curing agent, it partially replaced the sand used in the mixture. Because the densities of the sand and LWA are substantially different (Table 2), the ultimate substitution was performed on a volume basis. This means that the volume, of replaced sand was equal to the volume of incorporated LWA.

For Mix L-SAP where SAP was used as the internal curing agent, dry SAP powder was mixed with dry cement before adding water. The dosage of the SAP incorporated has been always reported as the mass of dry SAP divided by the mass of dry cement. However, in different studies, different dosages of SAP, from 0.3 wt.% to 0.6 wt.% [23]–[25], have been suggested to be incorporated to provide internal curing for concrete mixtures. For Mix L-SAP, the utilized SAP dosage was equal to 0.4 wt.%. In addition, the weight of additional water to the weight of SAP was equal to 25. This water was added to the mix water. Details regarding the proportioning for all the mixtures used are presented in Table 4. Considering the weights of the fine aggregate and LWA in Mix L-LWA and Mix Q-LWA, it can be concluded that for the purpose of internal curing, approximately 25 wt.% of the fine aggregate should be replaced by fine LWA (Table 4).

Table 4. Mixture proportioning (weight or volume of each ingredient in one yd³ of concrete)

Mixture ID	Mixture description	Coarse Agg. ¹ (lbs.)	Fine Agg. ¹ (lbs.)	Cement (lbs.)	Water (lbs.)	Internal curing agent		Additional water ² (lbs.)	Admixtures (fl. oz.)		
						LWA (lbs.)	SAP (lbs.)		AEA ³	SP ⁴	AA ⁵
Mix L-NIC	Limestone No IC ⁶	1,685	1,304	800	240	-	-	-	44	72	560
Mix Q-NIC	Quartz No IC ⁶	1,617	1,304	800	240	-	-	-	44	72	560
Mix L-SAP	Limestone + SAP	1,685	1,304	800	240	-	3.20	80.0	32	56	560
Mix L-LWA	Limestone + LWA	1,685	992	800	240	197	-	36.4	44	72	560
Mix Q-LWA	Quartz + LWA	1,617	992	800	240	197	-	36.4	44	72	560

¹ At oven-dry condition

² The additional water is stored in the porous structure of the carrier agent; thus, it would not change the water to cement ratio of the concrete mixture.

³ Air Entraining Admixture

⁴ Superplasticizer

⁵ Accelerating Admixture

⁶ Internal Curing

4.1.3 Test Methods

4.1.3.1 Fresh Concrete Properties

ASTM C143 “Standard Test Method for Slump of Hydraulic-Cement Concrete” was followed to measure the slump of all the concrete mixtures. Based on ASTM C928 “Standard Specification for Packaged, Dry, Rapid-Hardening Cementitious Materials for Concrete Repairs,” the targeted slump for all the mixtures was 3”. Air content of Mix L-NIC, Mix Q-NIC, and Mix L-SAP was measured using a pressure Type B meter, according to ASTM C231 “Standard Test Method for Air Content of Freshly Mixed Concrete by the Pressure Method.” However, this standard specifies that it is not applicable to concrete made with LWA. Therefore, for Mix L-LWA and Mix Q-LWA, which contain LWA, ASTM C173 “Standard Test Method for Air Content of Freshly Mixed Concrete by the Volumetric Method” was followed to measure the air content of the mixture. This

standard is specifically designed to determine the air content of concrete containing LWA by the volumetric method. The target air content for each mixture was 6% based on the Publication 408 specification.

4.1.3.2 Compressive Strength

ASTM C39 “Standard Test Method for Compressive Strength of Cylindrical Concrete Specimens” was followed for determining the compressive strength. After mixing, the concrete mixture was placed in 4" × 8" cylindrical molds. The molds then were covered with a wet burlap for 24 hours, and after demolding, the specimens were kept in an environmental room with constant temperature and humidity. Based on ASTM C157 “Standard Test Method for Length Change of Hardened Hydraulic-Cement Mortar and Concrete,” the air in the room was maintained at 73±3 °F, the relative humidity was maintained at 50±4%. It should be clarified here that the specimens were not moist-cured after demolding, and it was because of two main reasons: first, the goal of this test was to monitor the strength gain of repair material when they are cured in a manner similar to that of the field curing condition. In the field, when the repair material is placed, a curing compound is sprayed over the repair a few hours after placing, and no further curing is provided at higher ages. Therefore, after demolding, the specimens were not kept in a moist curing room. Second, the main goal of this project is to study the effects of internal curing on different characteristics of repair materials. Therefore, in order to have an accurate evaluation of the internal curing performance, the specimens were not exposed to external curing.

For each mixture design, twelve cylindrical specimens were prepared, with three specimens tested at the ages of 7-hours, 1-day, 7-days, and 28-days. Before testing, the specimens were capped with sulfur compound in accordance with ASTM C617 “Standard Practice for Capping Cylindrical Concrete Specimens” to ensure that the test cylinder had parallel, smooth, and uniform bearing surfaces that were perpendicular to the applied axial load during the test. The loading rate was 440 lbf/sec for all compressive strength specimens.

It should be mentioned that in order to provide a statistical interpretation of the experimental results, MINITAB software was used to apply the ANOVA and Tukey’s t-test for pairwise comparisons. Details regarding the statistical analysis are provide in the Appendix (Section 8).

4.1.3.3 *Modulus of Elasticity*

ASTM C469 “Standard Test Method for Static Modulus of Elasticity and Poisson's Ratio of Concrete in Compression” procedure was followed to measure the modulus of elasticity of specimens at 28 days. Based on the standard, the modulus of elasticity of concrete should be measured in the customary working stress range, which is 0 to 40% of the ultimate concrete strength. The three cylindrical samples which were prepared for the day-28 compressive strength were used for this test before they were broken for the compressive strength test. However, one extra sample was prepared and broken at the age of 28 days prior to conducting the elastic modulus test to measure the ultimate concrete strength. A compressometer, consisting of two yokes and two strain-gauges, was used to measure the deflection of the samples at different stress levels (Figure 7). Finally, the chord modulus of elasticity (E) of the concrete was calculated using the following equation:

$$E = \frac{S_2 - S_1}{\varepsilon_2 - 0.0006} \quad (2)$$

where S_2 is the stress corresponding to 40% of ultimate load (psi), S_1 is the stress corresponding to a longitudinal strain 0.0006" (psi), and ε_2 is longitudinal strain produced by stress S_2 . For each of the three specimens, the test was conducted at three different horizontal angles, and the average of the results was reported as the elastic modulus of concrete. The loading rate for all elastic modulus tests was 440 lbf/sec.

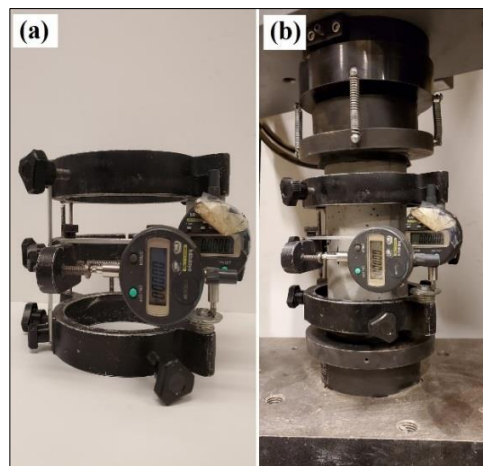


Figure 7. Elastic modulus test. a) Compressometer (Harness), b) Concreted specimen equipped with the compressometer, and under the compression machine

4.1.3.4 Bond Strength: Slant Shear

The bond shear strength between the in-situ concrete and the repair material is one of the key parameters that determine the service life of a partial depth repair section. In order to quantify the bond strength, a slant shear test was conducted based on ASTM C882 “Standard Test Method for Bond Strength of Epoxy-Resin Systems Used with Concrete by Slant Shear.” To do so, 2-year old 4" × 8" cylindrical concrete samples, which represent in-situ concrete, were cut at an angle of 30° from the vertical (Figure 8.a). Then, the slant shear specimen was made by casting the fresh concrete against the cut section contained in a specimen mold (Figure 8.b). For each mixture design, 6 specimens were prepared, with three specimens tested at the ages of 1 day and 28 days. Similar to the compressive strength test, the molds were covered with wet burlap for 24 hours, and after demolding, the specimens were kept in the environmental room. The air in the room was maintained at 73±3 °F, the relative humidity was maintained at 50±4%. The samples for the slant shear test were also capped with sulfur compound before testing.

To measure the bond shear strength, a compressive load was applied to the samples, and the bond strength was calculated by dividing the load carried by the specimen at failure by the area of the bonded surface, which was 25.12 in². Similar to the compressive strength test, the loading rate was 440 lbf/sec for all slant shear specimens.

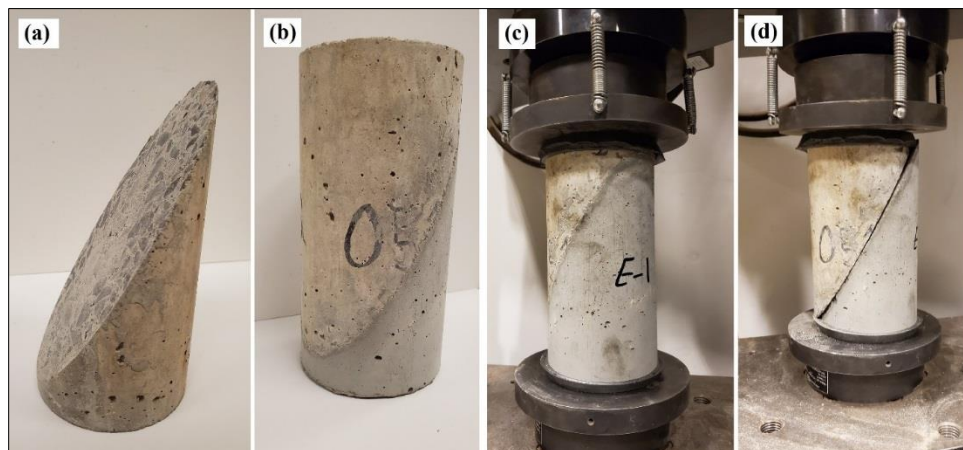


Figure 8. Slant shear test. a) Cut old specimen, b) Slant shear specimen after casting fresh concrete, c) Capped specimen under compressive force, d) Failed bond

4.1.3.5 Bond Strength: Splitting Tensile

Splitting tensile strength testing was conducted based on ASTM C496 “Standard Test Method for Splitting Tensile Strength of Cylindrical Concrete Specimens.” For this test, 2-year old 4" × 8" cylindrical concrete samples, which represent in-situ concrete, were cut in half along the length of the specimen (Figure 9.a). Then, the splitting tensile specimen was made by casting the fresh concrete against the cut section contained in a specimen mold (Figure 9.b). The molds were covered with a wet burlap for 24 hours, and after demolding, the specimens were kept in the environmental room at 73±3 °F and a relative humidity of 50±4%. For each mixture design, three specimens were prepared, which were tested at the age of 28 days.

To measure the bond strength, a diametral compressive force along the length of the cylindrical specimen was applied until failure of the bond. The bond strength was calculated using the following equation:

$$T = \frac{2 \times P}{\pi \times L \times D} \quad (3)$$

where T is the splitting tensile strength (psi), P is the maximum applied load (lb), L is the specimen length (in), and D is the specimen diameter (in). The loading rate for all splitting tensile specimens was 125 lbf/sec.

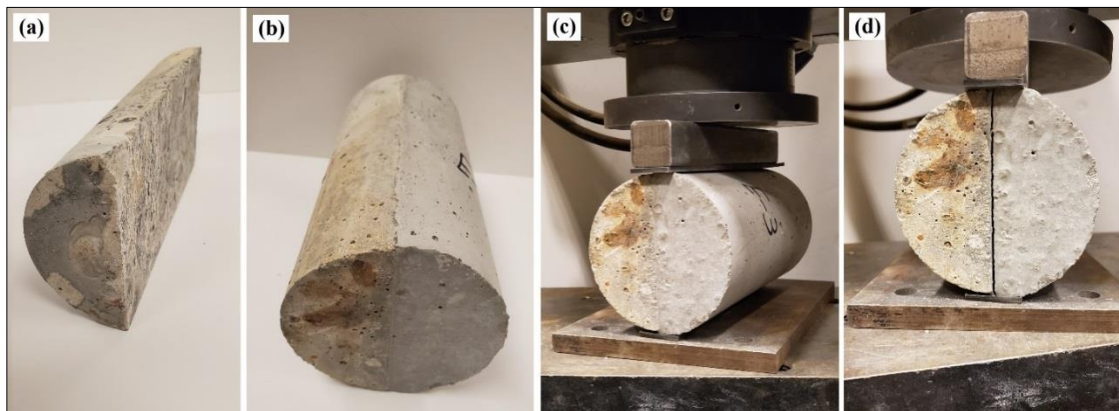


Figure 9. Splitting tensile test. a) Cut old specimen, b) Splitting tensile specimen after casting fresh concrete, c) Specimen under diametral compressive force (two rubber strips were used on the top and bottom of specimen to prevent stress concentration), d) Failed bond

4.1.3.6 Coefficient of Thermal Expansion

AASHTO T 336 “Standard Method of Test for Coefficient of Thermal Expansion of Hydraulic Cement Concrete” specification was followed to calculate the coefficient of thermal expansion (CTE) of concrete samples. The CTE of a saturated cylindrical concrete specimen was calculated by measuring the length change of the specimen due to change in temperature. Instead of using a linear variable differential transformer (LVDT), a vibrating wire strain gauge (VWSG) was used to measure the length change of the specimens (Figure 10.a).

To prepare the specimens, the VWSG was secured at the center of a 6" × 12" cylindrical mold using steel wires (Figure 10.b). Then the mold was gently filled with fresh concrete, and cured for 28 days. For each mixture design, two specimens were prepared, which were tested at the age of 28 days. The strain gauge used is a Model 4200 VWSG manufactured by GEOKON®. The VWSG had a length of 6", and was equipped with a plucking coil and a 10' connection cable (red cable in the figure). In order to record the responses, the connection cable was connected to a datalogger. The datalogger was a CR3000 Micrologger® manufactured by Campbell Scientific. The responses of the VWSG were recorded every 30 seconds. Based on AASHTO T 336, the CTE of the concrete specimens should be calculated by measuring the length change of specimen due to an increase in temperature, as well as a decrease in temperature. The specified temperature range is 50 °F to 122 °F. To do so, the concrete specimens were placed in a programmable water tank, which could apply a given temperature profile to the specimens (Figure 10.c).

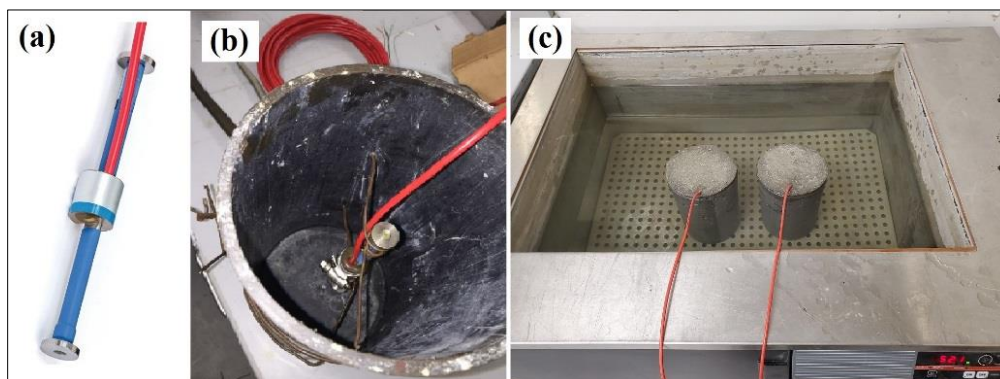


Figure 10. Coefficient of thermal expansion (CTE) test. a) Model 4200 vibrating wire strain gauge (VWSG), b) VWSG placed inside the mold, c) CTE samples inside the programmable water tank

The applied temperature profile is shown in Figure 11. The specimens were kept in the water tank at 50 °F for eight hours to stabilize the temperature. Then the temperature was slowly raised to 122 °F, and kept at this temperature for eight hours. Finally, the temperature was slowly reduced back to 50 °F, and was kept at this temperature for eight hours.

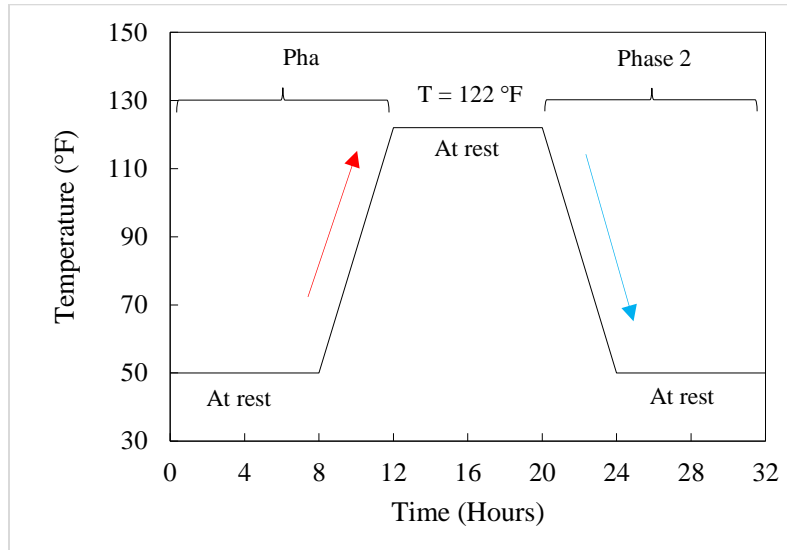


Figure 11. Applied temperature profile

Two parameters were measured using the VWSG: the vibration frequency of the coil and the temperature. The recorded frequency at each temperature was converted to strain using the equations provided in the VWSG manual. The CTE of the specimen was then calculated using the following equation:

$$CTE = \frac{\epsilon_2 - \epsilon_1}{T_2 - T_1} \quad (4)$$

where CTE is the coefficient of thermal expansion ($\mu\epsilon/^\circ\text{F}$), and ϵ_2 and ϵ_1 are the strains ($\mu\epsilon$) at the corresponding temperatures T_2 and T_1 ($^\circ\text{F}$), respectively. For each specimen, the CTE was calculated at two phases: phase 1, increase in temperature, and phase 2, decrease in temperature (Figure 11). Based on the standard, the value of the CTE calculated from both the increase and the decrease must be less than $0.2 \mu\epsilon/^\circ\text{F}$. The average of these two values is then reported as the CTE of the specimen.

4.1.3.7 Shrinkage

Total shrinkage testing was conducted based on ASTM C596 “Standard Test Method for Drying Shrinkage of Mortar Containing Hydraulic Cement.” For each mixture formulation, four specimens were prepared using 3" × 3" × 12" stainless steel prism molds (Figure 12.a). The molded samples were covered with wet burlap for 24 hours. Once demolded, samples were kept in the environmental room. Based on the ASTM C157 specifications, the air in the room was kept at a temperature of 73±3 °F, and a relative humidity of 50±4%. Measurements were taken on the day of demolding, every day for the first 7 days, and at the ages of 14 days, 21 days, and 28 days using a length comparator (Figure 12.b and c). The shrinkage at each age was calculated as:

$$Shrinkage(t) = -\frac{R(t) - R(0)}{L_0} \times 10^6 (\mu\epsilon) \quad (5)$$

where R(t) is the gauge reading at time t (in), R(0) is the gauge reading at the time of demolding (in), and L₀ is the length of comparator bar. It should be mentioned that based on the ASTM C596 specifications, once demolded, concrete specimens should be submerged in water to cure for 48 h, and then kept at room condition. However, the main goal to conduct this test was to measure the total shrinkage of the repair material when it is cured according to the actual field curing conditions. Therefore, submerging the specimens in water for 48 hours was not performed, and the specimens were kept in the environmental room at 73±3 °F and a relative humidity of 50±4% right after demolding. This more closely represents the actually curing conditions in the field, and therefore allows for a better of means of quantifying the effectiveness of internal curing, i.e. incorporating presoaked LWA and SAP, on controlling the shrinkage of repair materials.

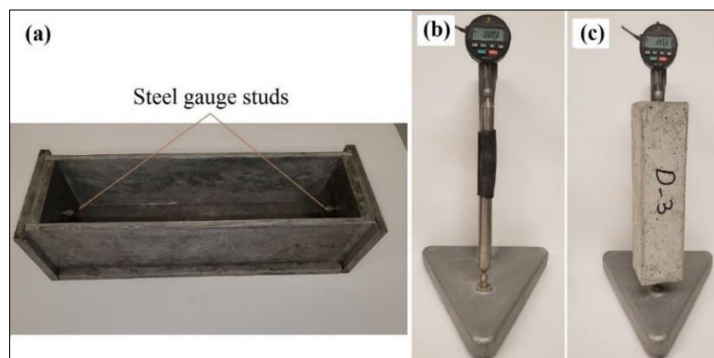


Figure 12. Shrinkage test. a) Steel prism mold, b) Length comparator with gauge, c) Specimen length change measurement

4.2 Results and Discussion of Laboratory Experiments

4.2.1 Compressive Strength

The results of the compressive strength test are depicted in Figure 13.

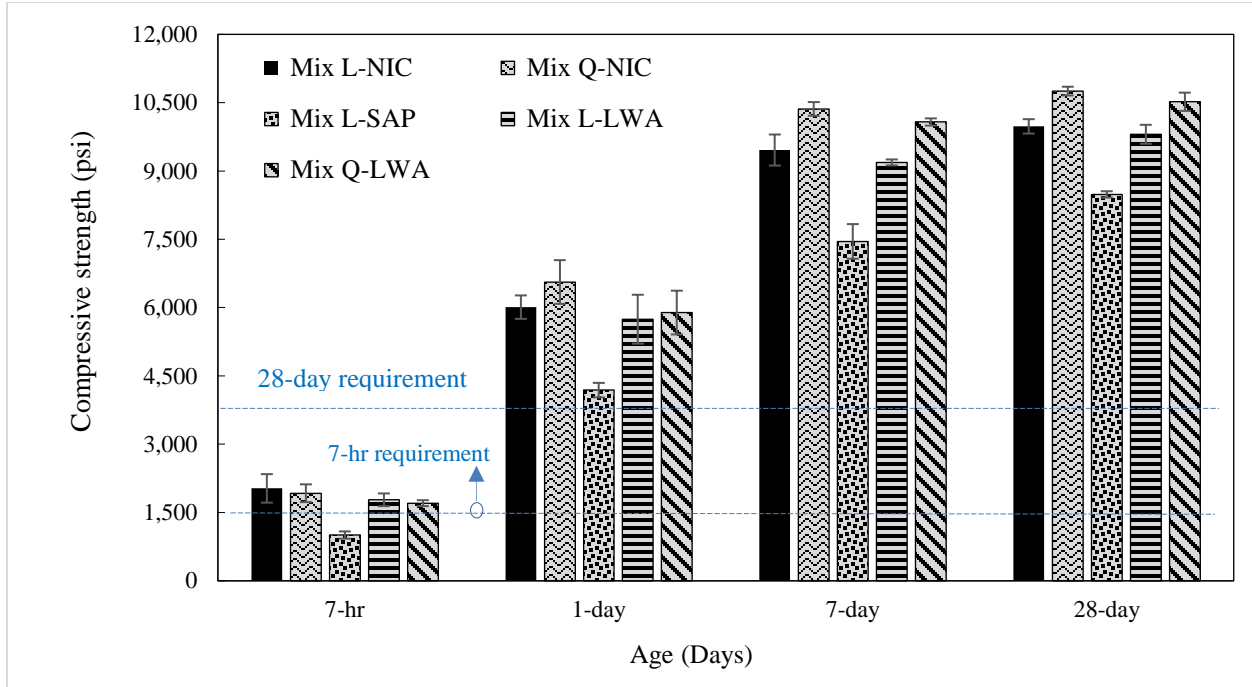


Figure 13. Compressive strength test

Based on the Publication 408 specifications, the required 7-hr compressive strength for Class AA Accelerated cement concrete repair materials is 1,500 psi. As the results show, all of the mixtures, except Mix L-SAP which contains SAP, meet the required 7-hr compressive strength. The average compressive strength for L-NIC, Q-NIC, L-LWA, and Q-LWA was 2,030 psi, 1,924 psi, 1,787 psi, and 1,706 psi, respectively. Comparing Mix L-LWA to Mix L-NIC, and Mix Q-LWA to Mix Q-NIC shows that incorporation of LWA reduces the 7-hr compressive strength by approximately 10%.

The required 28-day compressive strength specified by Publication 408 for Class AA Accelerated cement concrete repair materials is 3,750 psi. The results show that after 1 day, the compressive strength of all the mixtures, including Mix L-SAP, was higher than the required 28-day compressive strength. These results suggest that although the incorporation of LWA slightly

reduces the compressive strength, the concrete mixtures that contain LWA meet all the required compressive strength for Class AA Accelerated cement concrete repair materials.

The results also show that the incorporation of SAP as the internal curing agent significantly reduces the compressive strength. This finding is in accordance with the results presented in previous studies [25], [26]. The incorporation of SAP not only reduces the compressive strength, but also diminishes the strength gain rate of the mixture, and consequently delays the time to open the road to traffic.

The required compressive strength for Rapid-Set Concrete Patching Material class specified by Publication 408 Section 525 and ASTM C928 at the ages of 3 hr, 1 day, and 7 days are 1,000 psi, 3,000 psi, and 4,000 psi, respectively. The repair materials developed in this research do not meet the required 3-hr compressive strength requirements; therefore, they cannot be classified as Rapid-Set Patching Materials. However, as the results depicted in Figure 13 show, all the mixtures meet the 1-day and 7-day compressive strength requirements for the Rapid-Set Patching Materials.

The 28-day compressive strength of Mix L-NIC, Q-NIC, L-SAP, L-LWA, and Q-LWA was equal to 9,980 psi, 10,750 psi, 8,486 psi, 9,810 psi, and 10,220 psi. The high compressive strength of all the mixture designs is attributed to the high cement factor of the mixtures (800 lb/ft³). Comparing the results of Mix L-SAP to Mix L-NIC suggests that the incorporation of SAP reduces the 28-day compressive strength by approximately 15%. However, based on the statistical analysis, there is not a significant difference between the day 28 compressive strength of Mix L-LWA and L-NIC. This suggests that although fine LWA has a lower compressive strength than sand, because it provides internal curing and allows for the production of more hydration products during the curing time, it does not significantly reduce the compressive strength.

4.2.2 Modulus of Elasticity

The results of the elastic modulus test are depicted in Figure 14. Comparing the results of Mix L-NIC and Q-NIC reveals the effect of coarse aggregate on the elastic modulus of concrete. The mixture containing coarse limestone has a 28-day elastic modulus of 4,700,000 psi, whereas the mixture containing coarse quartzite has a 28-day elastic modulus of 4,200,000 psi.

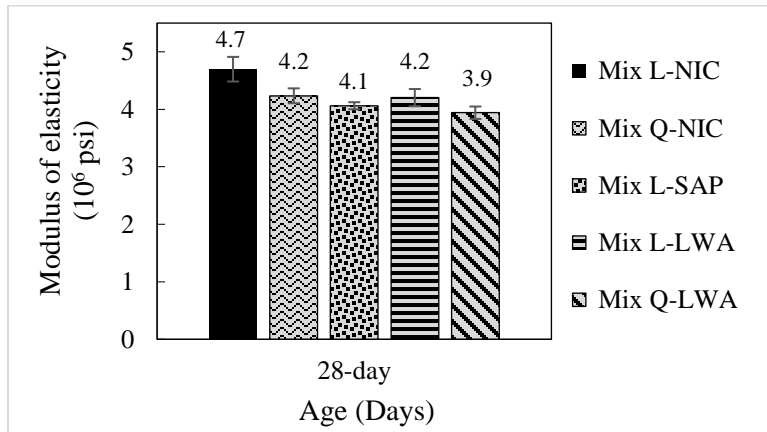


Figure 14. Modulus of elasticity test

Figure 15 depicts the effect of coarse aggregate elastic modulus on the concrete elastic modulus [27]. As it can be seen, in general, by increasing the elastic modulus of aggregate, the elastic modulus of concrete increases; however, there is not a linear relationship between these two parameters.

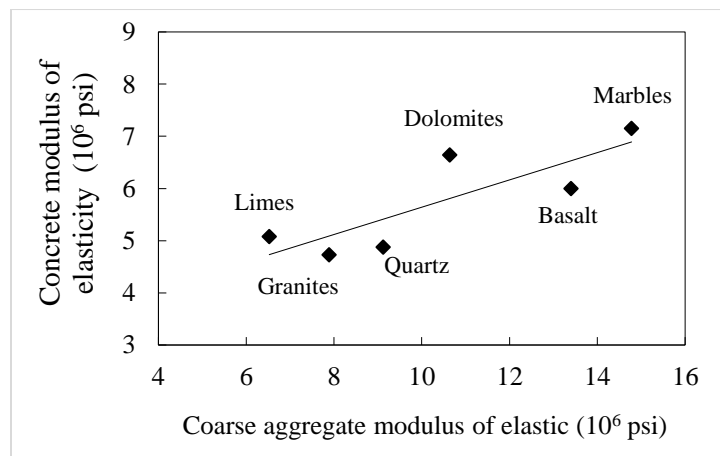


Figure 15. Effect of coarse aggregate type on concrete modulus of elasticity (adopted from [27])

The results of the elastic modulus test also suggest that the incorporation of internal curing agents, i.e. SAP and LWA, decreases modulus of elasticity of the concrete. For the case of SAP, the consumption of water that was stored in the SAP introduces voids to the cement paste bulk. For the case of LWA, since it is naturally less stiff than ordinary sand, the incorporation of the LWA resulted in a reduced elastic modulus of the concrete.

4.2.3 Bond Strength: Slant Shear

The results of the slant shear test are depicted in Figure 16. Publication 408 does not specify requirements for the bond strength of Class AA-Accelerated cement concrete repair materials. However, ASTM C928 requires the 1-day slant shear bond strength of Rapid-Set Patching Materials to be higher than 1,000 psi. As the results show, all the developed patching materials, including Mix L-SAP, meet this requirement.

The results of the statistical analysis suggest that the incorporation of LWA does not negatively affect the bond strength of repair materials. In addition, although the bond strength of Mix L-NIA is slightly higher than Mix Q-NIC, the results of the statistical analysis shows that there is not a significant deference between the slant shear bond strength of these two mixtures. This suggests that the coarse aggregate type included did not have a significant effect on the bond shear strength. The adhesive property of the cement paste plays the main role in the bond strength between the repair material and in-situ concrete, and this parameter is kept the same for all the mixtures. The incorporation of LWA did not significantly change the past strength; however, the incorporation of SAP as the internal curing agent decreased the day 28 slant shear bond strength of the repair material by approximately 15%. When measuring bond strength, the variability of results is usually large. Therefore, testing a larger number of samples would be more informative results.

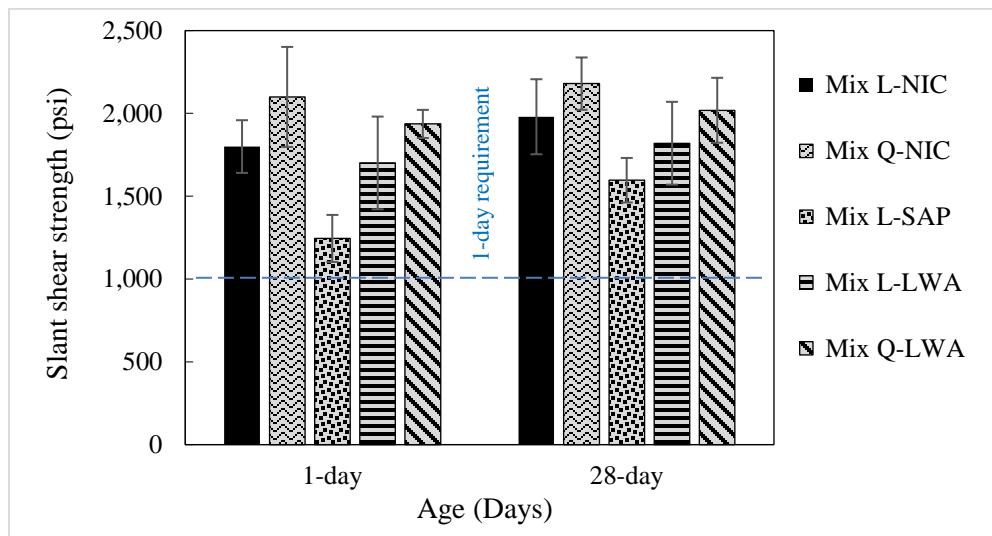


Figure 16. Slant shear bond strength test

4.2.4 Bond Strength: Splitting Tensile

In addition to the slant shear test, splitting tensile test was conducted on the samples to measure the bond strength between the repair material and the old concrete. Unlike the slant shear test, which evaluates the bond strength when it is subject to a combination of normal and shear stresses, splitting tensile test evaluates the bond strength when it is subjected to tensile strength (see Figures 8.d and 9.d for the failure mode of these two tests, respectively).

The results of the splitting tensile test are depicted in Figure 17. Publication 408 does not specify requirements for the splitting tensile bond strength of Class AA-Accelerated cement concrete repair materials. However, this test was conducted to evaluate the tensile mode of bond failure of the repair materials. Based on the results of the statistical analysis, neither changing the coarse aggregate type nor incorporating internal curing agent significantly the splitting tensile strength of the material. Similar to the slant shear test results, the variability of results in this test is large. Therefore, testing a larger number of samples makes it possible to drive more accurate and informative results.

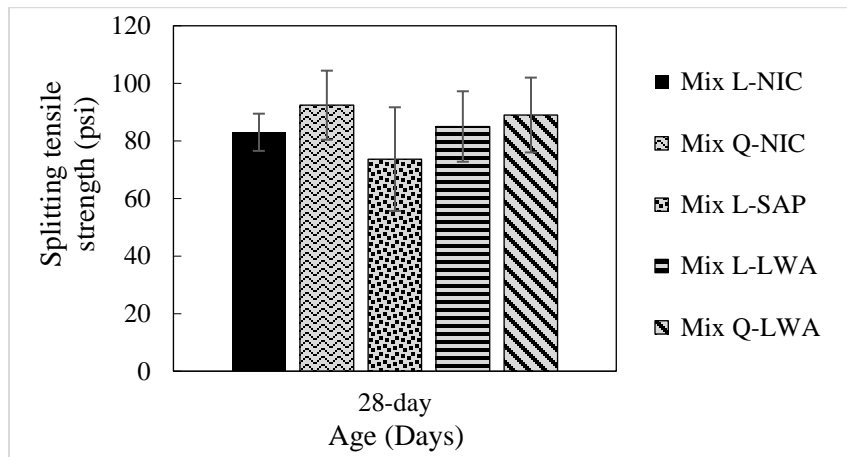


Figure 17. Splitting tensile test

Comparing the results of Figures 16 and 17 shows that the slant shear bond strength is approximately 20 times higher than the splitting tensile bond strength. This significant difference is attributed to the differences in stress distribution and failure modes between the two tests. In addition, similar to the slant shear test, the coarse aggregate type does not have a significant effect on the splitting tensile strength of repair material. This is because the main parameter that controls

the adhesive force between the two materials is the cement paste properties, which was kept constant for all the mixtures. In addition, the incorporation of internal curing agents did not significantly change the paste strength, either.

When it comes to interpreting the results of splitting tensile bond strength test and predicting the bond strength between concrete slab and repair section, three important points need to be considered:

- In the field, and due to the simultaneously applied thermal and mechanical loads, the bond face between the concrete slab and the repair section experiences a combination of shear, compressive, and tensile stresses. However, in this test, the bond interface experiences almost pure tensile stresses. Therefore, this test does not represent the actual stress distribution along the interface between the concrete slab and repair section.

- The boundary condition of a repair section in the field is different than the boundary condition of the repair material in this test. In the field, the connection between the bottom face of the repair section and the upper face of concrete slab restrains the lateral deformation of the vertical interfaces between the concrete slab and repair section. However, in this test, there is no support to restrain the lateral deformation of repair material (see Figure 9.c).

- The interface between the repair material and old concrete that was studied in this test was a saw-cut smooth surface without any texture (see Figure 9.a). However, a distressed concrete slab has a rough and textured surface, and the interface between the concrete slab and repair section is not a smooth surface. The mechanical bond provide by the surface texture of the repair area in the field can have a significant effect on increasing the bond strength between the two materials.

All of these considerations imply that the splitting tensile test performed significantly underestimates the bond strength between the concrete slab and repair material. In a laboratory study, the effect of five different types of surface textures on the splitting bond strength along the repair interface was examined [28]. The examined textures included: as cast without roughening, sand blasted, wire brushed, drilled holes, and grooved surfaces. It was shown that sand blasted and grooved surfaces had the best performance, where they increased the splitting bond strength by more than 200% compared to a specimen with an as cast surface [28]. In addition, it was shown that wire brushing and drilling holes could increase the bond strength by about 100%. These results

suggest that texturing the interface is one of the key parameters that could improve the bond strength between the repair material and in-situ concrete. In order to evaluate the effect of surface roughness of the bond strength, one splitting tensile test was performed on a concrete specimen with grooved surface. It was observed that compared to the saw-cut case, the bond strength was increased by about 200% when the surface of the in-situ concrete was textured.

4.2.5 Coefficient of Thermal Expansion

The results of the coefficient of thermal expansion (CTE) test are depicted in Figure 18. The CTE of Mix L-NIC was equal to 5.2 ($\mu\epsilon/^\circ\text{F}$), whereas for Mix Q-NIC it was equal to 6.6 ($\mu\epsilon/^\circ\text{F}$). Comparing the CTE of these two mixes shows that the CTE of concrete is strongly influenced by the aggregate type. Comparing the results for Mix L-LWA to L-NIC and Q-LWA to Q-NIC shows that the incorporation of LWA reduces the concrete CTE by approximately 5%. In addition, the comparison between Mix L-SAP and L-NIC shows that the incorporation of SAP decreases the CTE by approximately 15%. These results suggest that the incorporation of internal curing agents reduces concrete CTE, which is attributed to the voids that are introduced to the media.

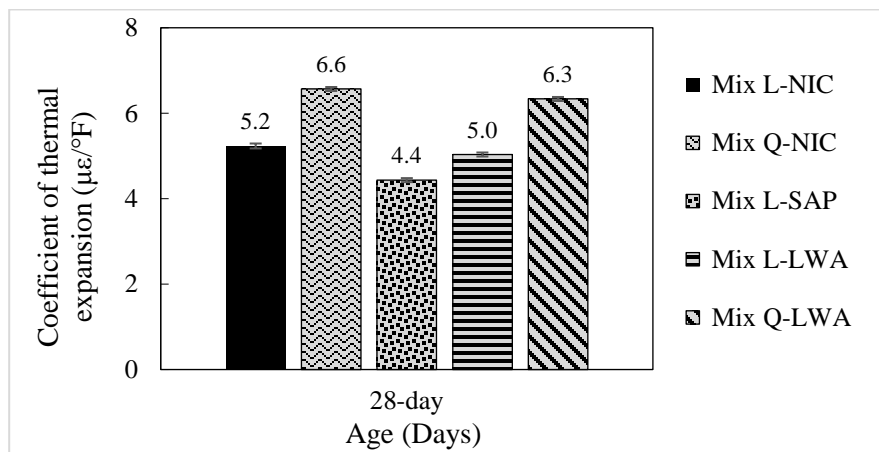


Figure 18. Coefficient of thermal expansion

The concrete CTE is also affected by the hardened paste content. The CTE of concrete (CTE_{PCC}) can be estimated using the CTE of the components [8]:

$$CTE_{PCC} = CTE_{agg} \times Vol_{agg} + CTE_{paste} \times Vol_{paste} \tag{6}$$

The CTE of hardened cement paste with a w/c of 0.4 to 0.6 is about 10 ($\mu\epsilon/\text{°F}$) [8]. Depending on the source, the CTE of typical aggregates varies between 2.3 ($\mu\epsilon/\text{°F}$) and 7.0 ($\mu\epsilon/\text{°F}$). Table 5 and Figure 19 provide the CTE of various types of aggregates, and concrete made of these aggregates [8].

Table 5. Typical CTE ranges for aggregates and, and the concrete made of these aggregates [8]

Aggregate type	Coefficient of thermal expansion ($\mu\epsilon/\text{°F}$)	Concrete coefficient of thermal expansion (made from this aggregate) ($\mu\epsilon/\text{°F}$)
Marbles	2.2 - 3.9	2.3
Limestones	2.0 - 3.6	3.4 - 5.1
Granites	3.2 - 5.3	3.8 - 5.3
Basalt	3.0 - 4.5	4.4 - 5.3
Dolomites	3.9 - 5.5	5.1 - 6.4
Sandstones	5.6 - 6.7	5.6 - 6.5
Quartz	5.5 - 7.1	6.0 - 8.7
Quartzite, Cherts	6.1 - 7.0	6.6 - 7.1

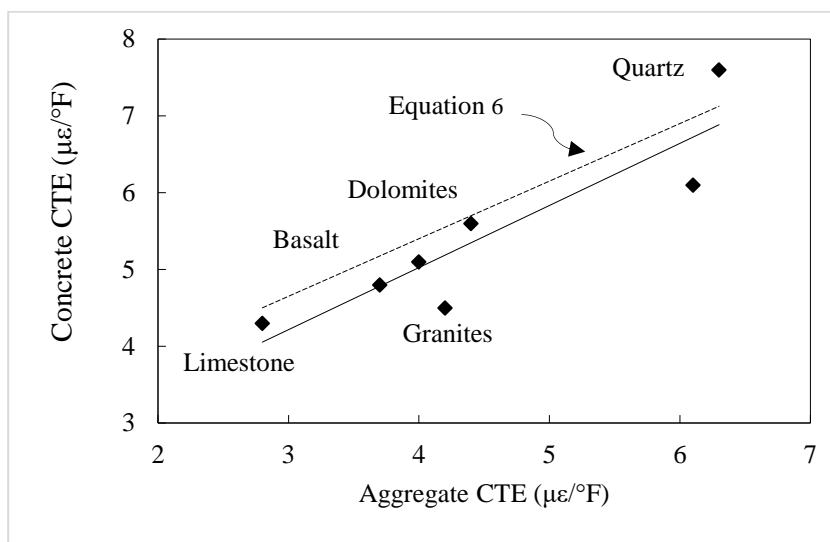


Figure 19. Effect of coarse aggregate type on concrete CTE (adopted from [8], [27])

4.2.6 Shrinkage

The results of the shrinkage test are depicted in Figure 20. The shrinkage of Mix L-NIC and Mix Q-NIC, where no internal curing agent was incorporated in the mixture, reached about 790 $\mu\epsilon$ after 28 days. However, when SAP was used as the internal curing agent, the shrinkages dropped to about 670 $\mu\epsilon$, and when presoaked LWA was used, it dropped to about 550 $\mu\epsilon$. The results provide evidence that internal curing significantly reduces the 28-day shrinkage of concrete. For the case of LWA, the shrinkage was reduced by approximately 30%, and for the case of SAP, the shrinkage was reduced by approximately 15% (Figure 20). This suggests that compared to SAP, LWA has a much better performance in reducing the shrinkage, which is in accordance with the results of previous studies.

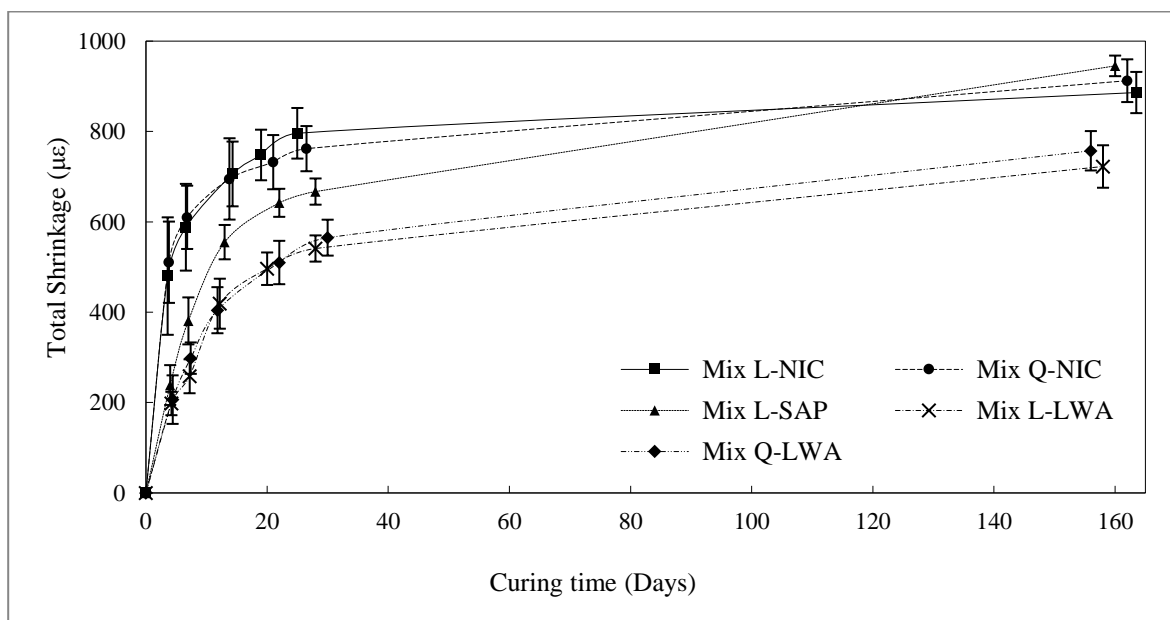


Figure 20. Shrinkage test

Table 6 presents a thorough comparison between the performance of SAP and LWA when used as internal curing agents. Compared to SAP, the negative effect of the incorporation of LWA on the compressive strength, modulus of elasticity, production of hydration products, and strength gain rate is less [29]–[31]. In addition, LWA is more effective in reducing shrinkage, and introduces less porosity to the bulk cement paste. These results suggest that when compared to SAP, LWA is a better internal curing agent for concrete.

Table 6. Comparison between the performance of SAP and LWA when used as internal curing agents

Criterion	Discussion	Source
Compressive strength	Incorporation of LWA yields a concrete with higher compressive strength compared to SAP.	[29]–[31]
Elastic modulus	Incorporation of LWA yields a concrete with higher stiffness compared to SAP.	[29]
Efficiency in reducing shrinkages	LWA provides greater relative reductions in autogenous shrinkage and drying shrinkage compared to SAP.	[29]–[31]
Effect on setting time	SAP produces a higher retardation of hydration reaction compared to LWA.	[29], [31]
Effect on porosity	While LWA reduces concrete’s porosity, the incorporation of SAP creates large amount of porosity along the interface between SAP and bulk cement paste.	[31]
Availability of prediction models for ultimate shrinkage	While a prediction model for ultimate shrinkage of concrete containing LWA is available, such a model for SAP-contained concrete is not available in the literature.	[32]

The drying shrinkage of concrete mixtures measured here were used as material inputs for the computational models developed for the numerical studies (Section 5). It should be mentioned that the values of shrinkage at the age of 28 days were used in the models since they were the most up-to-date available values when the numerical analysis were performed. However, at the end of project, one more set of measurements were made, which present the day 160 drying shrinkage. The new results show that after about five months, the drying shrinkage of concrete mixture containing SAP was statistically similar to that of control mixtures. This suggests that incorporating SAP as internal curing agent may not be an effective strategy to reduce the long-term shrinkage of repair materials. The results, however, suggest that for the mixtures that included

pre-soaked LWA as the internal curing agent, the long-term (five-month) shrinkage of concrete mixtures were up to 20% less than the control mixtures.

Nevertheless, there is an important point that needs to be considered when internal curing is used in concrete mixtures. Using internal curing delays the occurrence of drying shrinkage. For example, the mixtures that contain LWA reached to 750 $\mu\epsilon$ after 160 days, whereas the control mixtures reach to the same shrinkage level after only 14 days. For the first 14 days, the stiffness of concrete is low and the rate of creep is high. Both of these two factors reduce the generated stresses in the repair material at a similar shrinkage level. In other words, for mixtures with internal curing, the majority of the shrinkage might still occur, but at the time that the concrete is stiffer and the amount of creep is reduced. The other aspect of this is that the bond strength will also be increased at this later age. Further studies are required to fully understand and quantify the overall effect of internal curing on the long-term performance of repair materials. Developing a comprehensive model that takes into account the effect of internal curing in conjugation with the temporal effects of concrete creep, stiffness, and bond strength would be beneficial.

5 Numerical Modeling

A numerical evaluation of the MCR was conducted using the commercially available software ABAQUS. The model was used to conduct a detailed parametric study on the performance of various repair materials under different loading conditions. Any inconsistency between the mechanical and thermal properties of the repair material and in-situ concrete can decrease the performance life of the repair material by having a detrimental effect on the bond between the repair and in-situ concrete. Acquiring a comprehensive understanding of the detrimental effects resulting from the incompatibility between the repair and the existing concrete requires studying the effect of several parameters. This includes the difference between the material properties of the repair material and the in-situ concrete, loading scenarios, geometry of the repair and the pavement section, etc. Conducting such a thorough parametric study using laboratory experiments is expensive, time consuming, labor-intensive, and requires complex laboratory equipment. Therefore, these parameters will be investigated using a computational model that incorporates the material properties measured in the laboratory investigation.

5.1 Model Development

The finite element method was used to determine the stresses that are induced in the repair section and at the interface between the concrete slab and the repair. The general-purpose finite element software, ABAQUS was used for this analysis. An overview of the 3-D model developed for this investigation is shown in Figure 21. It consists of a slab on top of a base layer. The concrete slab was modeled as a 10" thick layer with the dimensions of 12' × 15'. The granular base was also 10" thick. The repair section was considered to be 3" thick layer with the dimensions of 20" × 30" (Figure 21). The mesh types used for the repair section, the concrete slab, and the base were a 20-node thermally coupled brick mesh, a 4-node thermally coupled tetrahedron mesh, and an 8-node thermally coupled brick mesh, respectively. The physical and thermal properties of the pavement layers are presented in Table 7. To validate the accuracy of the ABAQUS model, results obtained from the model were compared with previous studies [33]–[35].

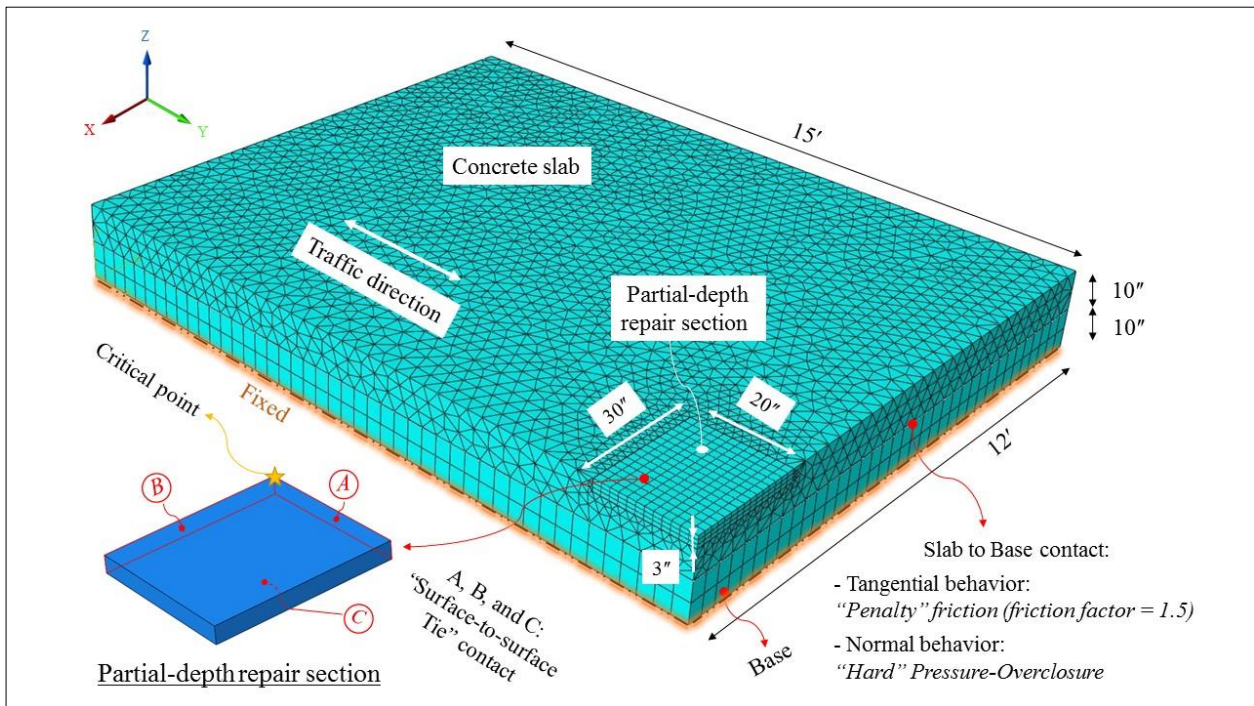


Figure 21. ABAQUS model: layers, contact surfaces, dimensions, critical stress point, and mesh (details regarding different load scenarios are provided in Section 5.2)

To study the effect of stiffness incompatibility and thermal incompatibility, two different values were chosen for the elastic modulus of the in-situ concrete and repair material, and two different values were chosen for the CTE of the in-situ concrete and repair material (Table 7). These values are the typical numbers for the concrete made with limestone and quartz coarse aggregate [8], [27]. The results from the laboratory part of this study fall in the same range.

Table 7. Physical and thermal properties of the pavement layers

Layer	Density (lb/ft ³)	E (psi)	CTE (μϵ/°F)	Drying shrinkage (μϵ)
Repair material	150	4,700,000 or 4,200,000	4.5 or 6.5	532 or 794
In-situ concrete	150	4,700,000 or 4,200,000	4.5 or 6.5	0
Base	120	25,000	4.0	0

5.2 Loading Scenarios

Five different load scenarios were studied. The load scenarios included:

1. Uniform changes in temperature;
2. Drying shrinkage;
3. Traffic load;
4. Uniform change in temperature and drying shrinkage; and
5. Uniform change in temperature, drying shrinkage, and traffic load. Details regarding each of the load scenarios are provided below.

Scenario 1: Uniform change in temperature

The change in length of a concrete slab due to uniform changes in temperature is a function of slab length, base/slab frictional factor, coefficient of thermal expansion of slab, and the magnitude of uniform temperature change [36]. The maximum range of uniform temperature change for the concrete slab was assumed to be equal to -70°F . This is the average daily minimum temperature in the city of Pittsburgh during the month of January (20°F) minus the temperature of the concrete at the time of placement (90°F) [36]. The friction between the bottom of the slab and the underlying base results in restraint of the elongation of the slab that will occur. The recommended friction factor for a granular base is 1.5 [37]. In the model, this value was used as the friction coefficient for the contact surface that was defined at the interface between the slab and the base layer. It should be mentioned that based on a sensitivity analysis, the normal stresses that were generated at the interface of the repair section and the in-situ concrete due to uniform changes in temperature were not sensible to the friction factor that was defined between the slab and the base.

Scenario 2: Drying shrinkage

Drying shrinkage was modelled by imposing a reduction in temperature to the repair material in the model. To do so, a decrease in temperature that would cause an equivalent decrease in length change due to drying shrinkage was applied to the repair section. This equivalent temperature change was calculated by dividing the total drying shrinkage by the CTE of repair material. Considering the values measured during the laboratory study and presented in Figure 20 (drying

shrinkage results), the equivalent temperature change for the case that no internal curing agent was incorporated in the concrete mixture was equal to $-122\text{ }^{\circ}\text{F}$ ($794\text{ }\mu\epsilon$ divided by $6.5\text{ }\mu\epsilon/^{\circ}\text{F}$). In addition, for the case where LWA was incorporated in the concrete mixture as the internal curing agent, this value was equal to $-82\text{ }^{\circ}\text{F}$ ($532\text{ }\mu\epsilon$ divided by $6.5\text{ }\mu\epsilon/^{\circ}\text{F}$). The calculated temperature change was applied only to the top surface of the repair section, and not to the entire concrete slab.

Scenario 3: Traffic load

The traffic load was simulated by applying an 18,000 lb single axle, which had four tires. The tire pressure was assumed to be 90 psi, which was applied over an $8\text{''} \times 6.25\text{''}$ rectangular area. Details regarding the traffic load dimensions and the location on the slab where the load was applied are depicted in Figure 22.

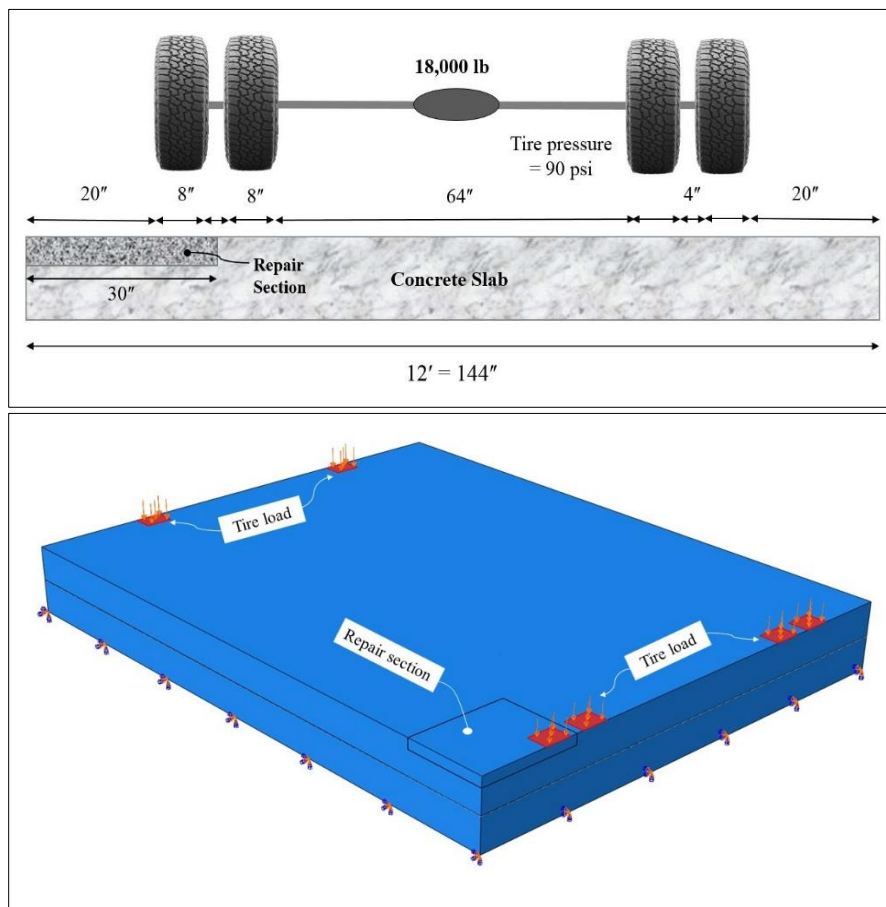


Figure 22. Traffic load

Scenario 4: Uniform change in temperature and drying shrinkage

This load scenario represents the case where the entire concrete slab experiences the average daily minimum temperature in January, and the repair section is subjected to a negative temperature gradient to capture the effects of drying shrinkage.

Scenario 5: Uniform change in temperature, drying shrinkage, and traffic load

This load scenario was similar to the previous load scenario, except the traffic load was added.

It should be mentioned that in addition to the aforementioned main loading scenarios, the slab was also studied when it was subjected to a temperature gradient. Negative temperature gradients (temperature of the upper surface of concrete slab is less than the bottom of the slab) develop during the nighttime. This temperature gradient causes upward curling, which leads to a loss of support at the slab corners [38]. Positive temperature gradients (the temperature of the surface of the concrete slab is higher than the bottom of the slab) occur during the afternoon. Positive temperature gradient causes downward curling, which leads to a loss of support at the center of slab. For a partial-depth repair located at the slab corner, the negative temperature gradient case is more critical; thus, the slab was studied under a negative temperature gradient loading condition. The temperature gradient applied was equal to -2 °F/in [39].

To capture the support loss due to temperature gradient, special consideration was given in the modeling. To do so, the displacement of the slab was not locked to the displacement of the base layer, and the normal behavior of the contact interface between the slab and the base was defined as “Linear Pressure-Overclosure.” This significantly increased the computational cost of the analysis. In addition, based on the modeling results, the stresses induced at the repair material due to the temperature gradient was negligible compared to the stresses induced due to other loading scenarios. Therefore, the temperature gradient through the slab’s thickness was not included in the studied loading scenarios.

5.3 Results and Discussion of Computational Simulations

Based on the computational simulations, the location of the critical tensile stress was slightly different for different load scenarios. However, for most of the scenarios, it took place at the intersection of Surface A and Surface B (Figure 21). Based on the preliminary simulations¹, tensile stresses developed at these interfaces were higher when a negative temperature gradient was applied to the concrete slab (compared to the case that a positive temperature gradient is applied). In addition, higher stresses occur when the CTE of repair section was higher than the CTE of concrete slab.

The normal stresses developed at interface between the concrete slab and repair section (Surface A and Surface B in Figure 21) were studied for different load scenarios. It should be mentioned that the tensile stresses at these interfaces were higher than the shear stresses at along the bottom surface of the repair. In addition, comparing the results of the slant shear test and the splitting tensile test suggests that shear strength is higher than tensile strength. Therefore, the focus of this study was on the tensile stresses at the interfaces (along surfaces A and B). To evaluate the effects of incompatibility between the in-situ concrete and repair section on the developed stresses, as well as the uncontrolled drying shrinkage, two scenarios were considered. For the first scenario, a material compatible repair (MCR) with internal curing, and for the second scenario, a conventional repair material without internal curing, were considered.

Details regarding the material properties of in-situ concrete and repair material for each of the load scenarios are provided in Table 8. For load Scenarios 1 and 3, and for the MCR scenario, the elastic modulus and CTE of in-situ concrete and repair section were considered to be equal, and no shrinkage was considered. For the same load scenarios, and for the conventional repair scenario, different values were considered for the elastic modulus and CTE of in-situ concrete and repair section, but still no shrinkage was considered. For load Scenario 2, and for the MCR scenario, the shrinkage for a concrete mixture with internal curing was considered; whereas for the conventional repair scenario, the shrinkage for a concrete mixture without internal curing was considered. For load Scenario 4, and for the MCR scenario, the elastic modulus and CTE of in-situ concrete and repair section were considered to be equal, and the shrinkage for a concrete mixture with internal

¹ Since it was not the main focus of this study, the results of this phase are not presented in this report.

curing was considered. However, for the conventional repair scenario, different values were considered for the elastic modulus and CTE of in-situ concrete and repair section, and the shrinkage for a concrete mixture without internal curing was considered. Load Scenario 5 was similar to load Scenario 4, except the traffic load was added to this load scenario.

Table 8. Material properties of the in-situ concrete and the repair material for different loading scenarios²

Load scenario	Description	Material compatible repair (MCR)					Conventional repair				
		E ₁ ¹	E ₂ ²	CTE ₁ ³	CTE ₂ ⁴	ε ⁵	E ₁ ¹	E ₂ ²	CTE ₁ ³	CTE ₂ ⁴	ε ⁶
1	Uniform ΔT: (1)	4.7	4.7	4.5	4.5	-	4.7	4.7	4.5	6.5	-
2	Shrinkage: (2)	4.7	4.7	4.5	4.5	532	4.7	4.7	4.5	4.5	794
3	Traffic load: (3)	4.7	4.7	4.5	4.5	-	4.7	4.2	4.5	4.5	-
4	(1) + (2)	4.7	4.7	4.5	4.5	532	4.7	4.2	4.5	6.5	794
5	(1) + (2) + (3)	4.7	4.7	4.5	4.5	532	4.7	4.2	4.5	6.5	794

¹ Modulus of elasticity of in-situ concrete (10⁶ psi)

³ Coefficient of thermal expansion of in-situ concrete (μϵ/°F)

⁵ Total shrinkage of repair material with internal curing (μϵ)

² Modulus of elasticity of repair material (10⁶ psi)

⁴ Coefficient of thermal expansion of repair material (μϵ/°F)

⁶ Total shrinkage of repair material without internal curing (μϵ)

² It should be clarified that although the incorporation of LWA slightly changes the elastic modulus and CTE of the repair materials (Figure 14 and Figure 18), these parameters were kept unchanged for the IC mixes in order to be able to study the net effect of each parameter separately.

The results of the stresses analysis are summarized in Table 9. This table presents the maximum tensile stress that developed at Surface A and Surface B (Figure 21) of the repair section for different load scenarios and material properties.

Table 9. Tensile stress along surfaces A and B of the repair

Load scenario	Description	Surface A: σ_x (psi)		Surface B: σ_y (psi)	
		MCR	Conventional repair	MCR	Conventional
1	Uniform ΔT : (1)	12	516	18	528
2	Shrinkage: (2)	808	1185	726	1089
3	Traffic load: (3)	-78	-81	108	114
4	(1) + (2)	625	1615	548	1516
5	(1) + (2) + (3)	608	1606	602	1584

- Surface A

The maximum tensile stress at this surface due to a uniform temperature change for the MCR was 9 psi, and 516 psi for the conventional repair. This suggests that because of thermal incompatibility of repair material, where the repair material CTE was 30% higher than the in-site CTE, the tensile stresses at the interface could significantly increase.

For load Scenario 2, the maximum tensile stress due to shrinkage was 808 psi for the MCR repair with internal curing, and 1,185 psi for the conventional repair. This shows the importance of incorporating internal curing agents in the repair materials. In addition, comparing the results of these three load scenarios suggests that the tensile stresses developed at the bond interface due to the concrete shrinkage are significantly higher than the developed stresses due to changes in temperature.

For load Scenario 3 where traffic load was applied, compression stresses developed at the bond surface, which was because of the positive Poisson’s ratio of concrete. The vertical pressure of tires causes lateral expansion of in-situ concrete and repair section, which leads to compression

stresses at the interface. It is also worth mentioning that there was not a significant difference between the resultant stresses for the MCR scenario and conventional repair scenario. This suggests that the stiffness compatibility between the in-site concrete and repair material is not as critical as thermal compatibility.

For load Scenario 4, and for the MCR with internal curing scenario, the maximum tensile stress at the bond surface was equal to 625 psi; whereas for the conventional repair without internal curing the stress was 1,615 psi (approximately 160% increase). Comparing these two values reveals the importance of the compatibility between the in-situ concrete and repair material, as well as the importance of incorporating internal curing agents in the repair material.

The stresses developed at the bond surface due to load Scenario 5 was almost equal to load Scenario 4. This suggests that as compared to shrinkage and thermal loads, traffic load is a less important parameter in developing tensile stresses at the interface.

- Surface B

The stresses developed at Surface B of the repair section under different load scenarios and material properties configurations were very similar to the stresses developed at Surface A, except for the case of the traffic load. For this load scenario, tensile stresses developed along Surface B. For the MCR scenario, the tensile stress was equal to 108 psi; whereas for the conventional repair, it was 114 psi.

The results for other load scenarios suggest that the thermal compatibility of the repair material and incorporating internal curing agents to control the shrinkage of the repair material significantly reduced the stress at the interface of in-situ concrete and repair material.

To better visualize the effect of thermal compatibility and internal curing on the stress that developed at Surface A and Surface B, the stresses are presented in the bar graph shown in Figure 23. At it can be seen, for load Scenario 6, the incompatibility between the repair and the existing concrete for the conventional repair material contributes to more than 60% of the total stress. These results show the importance of thermal compatibility between the in-situ concrete and repair material, as well as the importance of incorporating internal curing agents in the repair material to control the shrinkage.

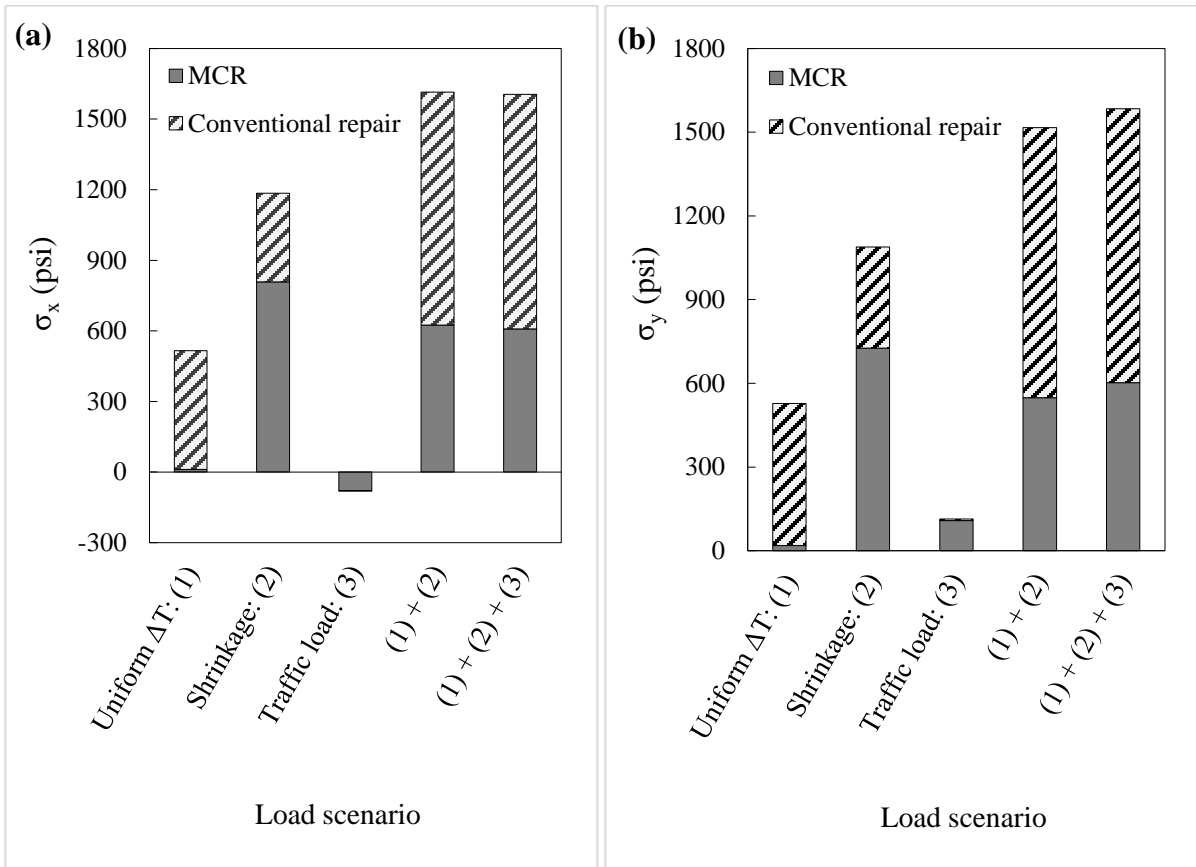


Figure 23. Stresses developed at a) Surface A and b) Surface B of the repair section under different load scenarios

6 Implementation Plan

6.1 Practical Considerations and Obstacles

In the previous sections, the importance of using MCRs was shown, best practices of developing a concrete mixture for an MCRs were discussed, and the performance of MCRs under different loading conditions were evaluated. It was also shown that using MCRs could reduce the stress that develops at the interface of concrete slab and repair section by 60%. However, there are some obstacles in regards to developing the mixture design for the MCR. They include the following:

- In order to develop a concrete mixture design for an MCR, the CTE of the existing concrete must be known. This can be established by pulling a core from the structure to be repaired and measuring the CTE directly. The CTE of the in-situ concrete can also be estimated based on the type of coarse aggregate used, similar to what is done when designing a pavement using Pavement ME.

- An LWA, or other material that can be used as an internal curing agent, might not be readily available for all project locations, although these types of products are becoming increasingly more available.

- Economics is also a consideration when considering the feasibility of using an MCR. A significant portion of the price of the coarse aggregate and LWA is the cost of transporting the material to the jobsite. Therefore, if the project location is far from the source of the required coarse aggregate and LWA, developing an MCR might not be economical.

The approximate cost of 7-hr-accelerated concrete repair material for a Pennsylvania project recently performed on the western side of the state was \$150 per cubic yard. An estimate of the cost breakdown for this mixture is provided in Table 10. For this project, the shipping cost of fine and coarse aggregate formed approximately 10% of the total cost of the mixture (Table 10).

Table 10. Cost breakdown of conventional accelerated concrete repair material and MCR (\$/yd³)

Item	Conventional repair material (\$/yd ³)	Note	MCR (\$/yd ³)
Cement	62	-	62
Coarse aggregate	27	\$16 material, \$11 shipping	27
Sand	9	\$4 material, \$5 shipping	6.5
Admixtures	22	-	22
Additional costs	30	Overhead, labor, operating costs, etc.	30
LWA	-	-	12.5
Sum	150	-	160

In most cases, the distance between the project and the aggregate source is was relatively short to minimize the aggregate shipping cost. However, when it comes to providing internal curing for the repair material, there might not be an LWA quarry sufficiently close to the project location. For this research effort, the cost of the LWA was \$60/ton, and the LWA hauling cost was approximately \$65/ton, since the location of the manufacturer was approximately 400 miles away from the project location. Thus, the incorporation of LWA would increase the total cost of concrete mixture by about 7%. A 7% increase in the cost of material is relatively minimal with respect to the total cost of a partial depth repair since these repairs are labor intensive. The process of performing partial depth repairs consists of cutting and preparing the repair section; applying the bonding epoxy; casting, finishing, and curing the repair material; and sealing the repaired section. Based on a preliminary cost analysis, the material accounts for only about 1% of the total cost of the repair. This suggests that the incorporation of LWA in the mixture would increase the total cost of the repair by less than 0.1%. It should be noted that this analysis only considers the increase in material costs and not additional costs accrued as a result of any additional handling/stockpiling of the additional materials.

6.2 Methodology for Developing a PERM for an MCR

An approach for developing the concrete mixture (which from here forward will be referred to as a performance engineered concrete repair mixture (PERM)) for the MCR is presented below. The approach developed for performance engineered mixtures (PEM) for concrete pavements was adopted here for PERMs [40]. The development of the PERM to be used for the MCR is critical to the performance of the MCR. Through this study, the key properties of repair material that will contribute to improved performance have been identified.

The two main steps toward developing a PERM are:

- Identifying the CTE of the in-situ concrete;
- Using appropriate materials and proportioning so
 - the CTE of the PERM and the in-situ concrete are comparable,
 - drying shrinkage of the PERM is minimized (internal curing can be beneficial),
 - Strength and durability requirements are met.

Table 11 (next page) shows the requirements for developing a PERM in a manner consistent with that for PEMs.

Table 11. Summary of mixture requirements for developing PERM

Mix Parameter	Property	Specified test(s)	Acceptance
Cement	-	-	ASTM C150
Aggregate properties	Coarse aggregate	-	ASTM C33
	Fine aggregate	-	ASTM C136 / ASTM C778
	Lightweight aggregate	-	ASTM C330
Mixture design specifications	w/c	-	Pub 408-Section 704
	Cement factor	-	Pub 408-Section 704
	Coarse aggregate content	-	Pub 408-Section 704
Fresh concrete	Slump	ASTM C143	ASTM C928
	Air content	ASTM C231/ASTM C173	ASTM C928
	Setting time	ASTM C191	ASTM C928
	Mixing room condition	-	ASTM C511
Hardened concrete	Compressive strength	ASTM C39	Pub 408-Section 704/ASTM C928
	Flexural strength	ASTM C78	-
	Rapid chloride permeability	AASHTO T277	-
Bond strength	Slant shear	ASTM C882	ASTM C928
	Splitting tensile	ASTM C496	-
Compatibility	Coefficient of thermal expansion	AASHTO T 336	Material compatible repairs
	Internal curing	ASTM C1761	Material compatible repairs
	Shrinkage	ASTM C596	Material compatible repairs

7 Conclusion and Future Work

Partial-depth repairs are between commonly used concrete pavement and bridge deck rehabilitation methods. However, compared to other rehabilitation techniques such as full-depth repair, partial-depth repairs have a limited service life. Incompatibility between the in-situ concrete and repair material is one of the key parameters that can contribute to a shorter repair life. Therefore, in order to improve the performance of the repair section, it is critical to perform a material compatible repair using a PERM with controlled shrinkage. Doing so increases the service life of the repair, improves the ride quality, increases safety, decreases closure time, and reduces costs and material consumption. In this study, it was first shown that stiffness compatibility, thermal compatibility, and controlled shrinkage are the main three compatibility properties for an MCR. Then through a comprehensive laboratory study, it was shown that coarse aggregate type is the key parameter to achieve stiffness and thermal compatibility. In addition, it was shown that the incorporation of presoaked lightweight aggregate (LWA) is a promising strategy to control the shrinkage of repair materials. Finally, by conducting computational modeling, it was shown that using a compatible material could reduce the induced stresses in the repair section by more than 60%. This study aimed to shed light on the importance of using MCRs, best practices to develop MCRs, and evaluate the performance of MCRs. However, more studies need to be conducted to better understand the properties and the performance of MCR under different conditions. Therefore, following are the suggested as future work:

- Developing a test procedure to accurately evaluate the effect of internal curing on the bond strength between in-situ concrete and repair material.
- Developing a comprehensive model that takes into account the temporal effects of the drying shrinkage, creep, stiffness, and bond strength when using internal curing.
- Studying the bond strength of MCR under cyclic loading (fatigue performance of the bond).
- Evaluating the effectiveness of using bonding agents on improving the bond strength.
- Conducting more computational modeling to evaluate the performance of MCR when they are used at different spots of a concrete slab (edge, center, etc.), have irregular geometry (close to the field conditions), or have different boundary conditions (effect of dowel bars, etc.).

- Improving the accuracy of the computational models for the bond between the in-situ concrete and repair section.
- Conduct and investigation to establish the long-term cost effectiveness of using MCRs.

8 Appendix (Statistical Analysis Details)

In order to provide a statistical interpretation of the experimental results, MINITAB software was used to apply Analysis of Variance (ANOVA) and Tukey’s test for pairwise comparisons. The significance level was selected to be equal to 0.05, which yields confidence level of 95%. Table 12 and Table 13 present the results of statistical analysis for the laboratory tests. These tables basically compare the results of different mixes for a given test at a specific age. Falling in the same category, i.e. A, B, or C, simply means that the results are not significantly different. However, if the results fall in different categories, they are significantly different.

Table 12. Statistical analysis of the compressive strength test at different ages

Mixture ID	Age			
	7-hr	1-day	7-day	28-day
L-NIC	A	A	A	A
Q-NIC	A	A	B	B
L-SAP	B	B	C	C
L-LWA	A	A	A	A
Q-LWA	A	A	B	B

Table 13. Statistical analysis of the other tests at age 28-day

Mixture ID	Test				
	Elastic modulus	Slant shear	Splitting tensile	CTE	Shrinkage
L-NIC	A	A	A	A	A
Q-NIC	B	A	A	B	A
L-SAP	B	A	A	C	B
L-LWA	B	A	A	D	C
Q-LWA	B	A	A	E	C

9 References

- [1] D. Frentress and D. Harrington, “Partial-depth repairs for concrete pavements,” CP Road Map, MAP Brief 7-2, 2011.
- [2] PennDOT, *Publication 408: Specifications*. Harrisburgh, PA: Pennsylvania Department of Transportation, 2018.
- [3] PennDOT, *Publication 242: Pavement Policy Manual*. Harrisburgh, PA: Pennsylvania Department of Transportation, 2018.
- [4] PennDOT, *Publication 55: Bridge Maintenance Manual*. Harrisburgh, PA: Pennsylvania Department of Transportation, 2002.
- [5] T. P. Wilson, K. L. Smith, and A. R. Romine, “Materials and Procedures for Rapid Repair of Partial-Depth Spalls in Concrete Pavements: Manual of Practice,” Federal Highway Administration, Washington, D.C., FHWA-RD-99-152, 1999.
- [6] PennDOT, “PennDOT Meeting Research Ideas 12-8-16.” Pennsylvania Department of Transportation, 2016.
- [7] A. Valikhani, A. J. Jahromi, I. M. Mantawy, and A. Azizinamini, “Experimental evaluation of concrete-to-UHPC bond strength with correlation to surface roughness for repair application,” *Construction and Building Materials*, vol. 238, p. 117753, 2020.
- [8] NCHRP, “Guide for Mechanistic-Empirical Design of New and Rehabilitated Pavement Structures,” 2004. .
- [9] D. P. Bentz and Weiss, W.J., “Internal Curing: A 2010 State of the Art Review,” National Institute of Standards and Technology (NIST), Gaithersburg, MD, NISTIR-7765, 2011.
- [10] J. Weiss, “Internal Curing for Concrete Pavements,” Federal Highway Administration, Washington, D.C., FHWA-HIF-16-006, 2016.
- [11] J. Qian, C. You, H. Wang, and X. Jia, “A Method for Assessing Bond Performance of Cement-Based Repair Materials,” *Construction Building Materials*, vol. 68, pp. 307–313, 2014.
- [12] J. Castro, I. De la Varga, M. Golias, and W. Weiss, “Extending internal curing concepts to mixtures containing high volumes of fly ash,” in *International Bridge Conference*, 2010.
- [13] T. Barret, A. Miller, and W. J. Weiss, “Documentation of the INDOT Experience and Construction of Bridge Decks Containing Internal Curing,” Indiana Department of Transportation, Indianapolis, IN, 2015.
- [14] EPA, “Lightweight Aggregate Manufacturing,” in *AP-42: Compilation of Air Emissions Factors*, Washington, D.C.: Environmental Protection Agency, 2016.
- [15] M. Aslam, P. Sha, M. Zamin, and M. Lachemi, “Benefits of Using Blended Waste Coarse Lightweight Aggregates in Structural Lightweight Aggregate Concrete,” *Journal of Cleaner Production*, vol. 119, pp. 108–117, 2016.
- [16] M. Golias, J. Castro, and J. Weiss, “The Influence of the Initial Moisture Content of Lightweight Aggregate on Internal Curing,” *Construction Building Materials*, vol. 35, pp. 52–62, 2012.
- [17] J. Kevern and C. Farney, “Reducing Curing Requirements for Pervious Concrete with a Superabsorbent Polymer for Internal Curing,” *Transportation Research Record Journal of the Transportation Research Board*, vol. 2290, no. 1, pp. 115–121, 2012.

- [18] J. Justs, M. Wyrzkowski, D. Bajare, and P. Lura, “Internal Curing by Superabsorbent Polymers in Ultra-High Performance Concrete,” *Cement Concrete Research*, vol. 76, pp. 82–90, 2015.
- [19] S. Kawashima and S. P. Shah, “Early-Age Autogenous and Drying Shrinkage Behavior of Cellulose Fiber Reinforced Cementitious Materials,” *Cement Concrete Composites*, vol. 33, no. 2, pp. 201–208, 2011.
- [20] D. P. Bentz, P. Lura, and J. W. Roberts, “Mixture proportioning for internal curing,” *Concrete international*, vol. 27, no. 2, pp. 35–40, 2005.
- [21] N. P. Sharifi, H. Jafferji, S. E. Reynolds, M. G. Blanchard, and A. R. Sakulich, “Application of lightweight aggregate and rice husk ash to incorporate phase change materials into cementitious materials,” *Journal of Sustainable Cement-Based Materials*, vol. 5, no. 6, pp. 349–369, 2016.
- [22] T. Merzouki, M. Bouasker, N. E. H. Khalifa, and P. Mounanga, “Contribution to the modeling of hydration and chemical shrinkage of slag-blended cement at early age,” *Construction and Building Materials*, vol. 44, pp. 368–380, 2013.
- [23] O. M. Jensen and P. F. Hansen, “Water-entrained cement-based materials: II. Experimental observations,” *Cement and Concrete Research*, vol. 32, no. 6, pp. 973–978, 2002.
- [24] V. Mechtcherine, “Use of superabsorbent polymers (SAP) as concrete additive,” *RILEM Technical Letters*, vol. 1, pp. 81–87, 2016.
- [25] A. M. Soliman and M. L. Nehdi, “Effect of drying conditions on autogenous shrinkage in ultra-high performance concrete at early-age,” *Materials and Structures*, vol. 44, no. 5, pp. 879–899, 2011.
- [26] X. Kong, Z. Zhang, and Z. Lu, “Effect of pre-soaked superabsorbent polymer on shrinkage of high-strength concrete,” *Materials and Structures*, vol. 48, no. 9, pp. 2741–2758, 2015.
- [27] D. P. Bentz *et al.*, *Influence of aggregate characteristics on concrete performance*. US Department of Commerce, National Institute of Standards and Technology, 2017.
- [28] B. A. Tayeh, B. A. Bakar, M. M. Johari, and Y. L. Voo, “Evaluation of bond strength between normal concrete substrate and ultra-high performance fiber concrete as a repair material,” *Procedia Engineering*, vol. 54, pp. 554–563, 2013.
- [29] D. P. Bentz, S. Z. Jones, M. A. Peltz, and P. E. Stutzman, *Influence of internal curing on properties and performance of cement-based repair materials*. US Department of Commerce, National Institute of Standards and Technology, 2015.
- [30] G. R. de Sensale and A. F. Goncalves, “Effects of fine LWA and SAP as internal water curing agents,” *International Journal of Concrete Structures and Materials*, vol. 8, no. 3, pp. 229–238, 2014.
- [31] B. A. Graybeal, C. A. Nickel, J. F. Munoz, R. P. Spragg, and I. De la Varga, “Application of Internal Curing in Cementitious Grouts for Prefabricated Bridge Concrete Elements Connections,” *Advances in Civil Engineering Materials*, vol. 7, no. 4, 2018.
- [32] H. Costa, E. Júlio, and J. Lourenço, “New approach for shrinkage prediction of high-strength lightweight aggregate concrete,” *Construction and Building Materials*, vol. 35, pp. 84–91, 2012.

- [33] V. Faraggi, C. Jofré, and C. Kraemer, “Combined effect of traffic loads and thermal gradients on concrete pavement design,” *Transportation Research Record*, vol. 1136, pp. 108–118, 1987.
- [34] H. T. Yu, L. Khazanovich, M. I. Darter, and A. Ardani, “Analysis of concrete pavement responses to temperature and wheel loads measured from instrumented slabs,” *Transportation Research Record*, vol. 1639, no. 1, pp. 94–101, 1998.
- [35] N. P. Sharifi and K. C. Mahboub, “Application of a PCM-rich concrete overlay to control thermal induced curling stresses in concrete pavements,” *Construction and Building Materials*, vol. 183, pp. 502–512, 2018.
- [36] “Superseded: Technical Advisory T 5040.30 Concrete Pavement Joints - Pavements - Federal Highway Administration.” [Online]. Available: <https://www.fhwa.dot.gov/pavement/t504030.cfm>. [Accessed: 09-Dec-2019].
- [37] Aa. Highway and T. Officials, *AASHTO Guide for Design of Pavement Structures, 1993*. Aashto, 1993.
- [38] H. T. Yu, L. Khazanovich, and M. I. Darter, “Consideration of JPCP curling and warping in the 2002 design guide,” in *83rd Annual Meeting of the Transportation Research Board, Washington, DC, 2004*.
- [39] S. Nassiri, “Establishing permanent curl/warp temperature gradient in jointed plain concrete pavements,” PhD Thesis, University of Pittsburgh, 2011.
- [40] “Performance Engineered Mixtures (PEM) for Concrete Pavements, Federal Highway Administration National Concrete Consortium. MAP Brief April 2017.”